FFI-RAPPORT

17/00141

Literature review on estimating ice thickness

—

Tonje Nanette Arnesen Hannevik

Literature review on estimating ice thickness

Tonje Nanette Arnesen Hannevik

Norwegian Defence Research Establishment (FFI) 19 December 2017

Keywords

Syntetisk apertur-radar (SAR)
Is
Refleksjon
Polarisasjon
Satellitter

FFI-rapport
FFI-RAPPORT 17/00141

Prosjektnummer
1441

ISBN
P: 978-82-464-2990-8
E: 978-82-464-2991-5

Approved by
Richard B. Olsen, *Research Manager*
Johnny Bardal, *Director*

Summary

This report is a literature review on how to estimate ice thickness using satellite altimeter and satellite SAR. A presentation is given on ice, the properties of ice and on how sea ice and the ocean reflect back to the SAR satellite. It is important to have knowledge of the sea ice volume, sea ice export, and of how the ice varies inter-annually due to climate changes, as well as oil and gas exploitation, ship traffic, and new ship routes in the north.

Much research has been done on how to estimate the sea ice freeboard using a satellite altimeter, for example ICESat and CryoSat-2. Some of the results show good agreement with in situ measurements. The data show a decline in the sea ice volume in the Arctic over many years.

Many different attempts have been made to estimate the sea ice thickness using satellite SAR. It has been claimed that it is impossible to estimate the sea ice thickness using SAR alone. Trials have been done to estimate the sea ice thickness by using satellite SAR. Some background information is necessary to be able to estimate the sea ice thickness by using SAR. It is for example necessary to localize areas with thin ice before it is possible to estimate the sea ice thickness. Many of the trials that have been done to estimate the sea ice thickness with SAR have been successful, but the estimates have been done within a certain thickness range where the approximate sea ice thickness is known in advance. If different methods are used to estimate the thickness of thin and thick ice, the chances are better to get the sea ice thickness estimate correct.

Sammendrag

Denne rapporten er et litteraturstudie om hvordan en kan beregne tykkelsen på sjøis ved å bruke altimeter (høydemåler) på satellitt og satellitt-SAR (syntetisk apertur-radar). Rapporten presenterer sjøis og egenskapene til sjøis, og gir en gjennomgang av hvordan sjøis reflekterer radarstråler tilbake til radaren. Det er viktig å ha kunnskap om sjøisvolumet og sjøiseksporten ut av Arktis, og kunnskap om hvordan sjøisen varierer fra år til år slik at en kan følge med på virkninger av klimaforandringer, olje- og gassutnytting, skipstrafikk og nye sjøruter på grunn av smelting av isen i nord.

Det er blitt forsket mye på hvordan en kan beregne istykkelsen ved hjelp av satellittaltimeter, for eksempel ICESat og CryoSat-2. Noen av resultatene viser god overenstemmelse med målinger på stedet. Dataene viser en minking av sjøisvolumet i Arktis over mange år.

Forsøk har også blitt gjort på å estimere sjøistykkelsen ved å bruke satellitt-SAR. Det hevdes at det er umulig å beregne sjøistykkelsen bare ved hjelp av SAR. Det trengs noe bakgrunnsinformasjon for å kunne beregne sjøistykkelsen med SAR. Det er for eksempel nødvendig å lokalisere områder med tynn is før en kan beregne sjøistykkelsen. Mange av forsøkene på å beregne sjøistykkelsen med SAR har vært vellykkede, men det er estimater som er gjort innenfor en viss tykkelseområde der den omtrentlige tykkelsen er kjent på forhånd. Blir det for eksempel brukt forskjellige metoder for å beregne tykkelsen av tynn og tykk is, vil det være større sjanse for at estimatet av sjøistykkelsesen blir riktig.

Content

1 Introduction

The Arctic sea ice has experienced a decline in recent years, and thus it is important to get an analysis of sea ice volume export discriminates between the thermodynamic, due to increased warming, and dynamic, due to increased export forcing. There are also undiscovered gas and oil reserves in the Polar Regions. Knowledge about the ice is also important to do ice management and to plan ship traffic. New routes open up in the north when the ice declines. In addition, the sea ice is important for climate change and thus a good knowledge of the ice's mass balance is crucial.

Earlier passive microwave sensors were used to do sea ice observations from space. Now satellite altimetry and SAR satellites are used to estimate and predict the ice volume in the Arctic. The data is validated using in situ data from ships, ice stations, upward looking sonars moored to the ocean floor and helicopters.

This report will first give a brief presentation about ice and some of the properties of ice in chapter 2. Chapter 3 will present surface and radar reflection from ice, snow and water using SAR data. Research on how to estimate sea ice freeboard and then the sea ice thickness is presented in chapter 4, while chapter 5 goes through different methods of estimating sea ice thickness using SAR in one polarization, as well as using dual- or quad-polarization. Chapter 6 describes how for example Canada, US, Finland and Norway do operational estimation of ice thickness. Conclusion and recommendations are given in chapter 7.

2 Ice

When the ocean is frozen, the microwave reflection mechanisms are changed. The ice differs in roughness, strength, salinity and thickness [www.nrgan.gc.ca]. Pack ice and ice floes are different ice types packed together and they are intersected by dynamic leads or cracks.

Table 2.1 Ice stages of ice development.

New: Smooth and thin. Newly formed ice crystals weakly frozen together. Least resistance to ice breakers.	Frazil: Fine plates or needles of ice separate from each other in the water Grease: Later freezing stage than frazil. The ice crystals have formed a soupy, dark, greasy layer on the surface. It is also called ice fat or lard ice. Slush: Snow mixed with water floating in water in a viscous surface layer after for example a heavy snow fall Shuga: Made of grease ice, slush or anchor ice rising to the surface. Collection of spongy white ice lumps with diameter of a few centimeters or more.
Nilas: Thin elastic crust of ice. Less than 10 cm thick. Bends easily on waves, often with striped or chevron appearance.	Dark nilas: Dark in color and up to 5 cm in thickness. Light nilas: Lighter than dark nilas in color and between 5 and 10 cm in thickness. Ice rind: Thickness of about 5 cm. Made by direct freezing or from grease ice on a quiet surface. Fragile, shiny crust of ice.
Young: Ice in the stage between Nilas and first-year ice. Thickness: 10-30 cm.	Grey ice: Thickness: 10-15 cm. Usually rafts under pressure (one layer over another), less elastic than nilas and breaks on swell. Grey-white ice: Thickness: 15-30 cm. Probably buckles to form ridges (on the edges) under pressure or collisions.
First-year ice: Sea ice younger than one winter, 30 cm or thicker.	First-year thin/white ice first-stage: 30-50 cm thick. Without ridges or deformations. First-year thin/white ice second-stage: 50-70 cm thick. Without ridges or deformations. First-year medium: 70-120 cm thick First-year thick: > 120 cm thick
Old or Multi-year: Ice of any thickness that has survived at least one summer melting season. It is generally smoother than first-year ice topographically. Undulating, weathered ridges.	Second-year ice: Ice that has survived one summer’s melt. It stands higher out of the water and it is thicker than first-year ice. During the summer, many small puddles in a regular pattern are produced, which are greenish-blue. Multi-year ice: Ice that has survived at least two summer’s melt. Hummocks are smoother and it is almost salt-free. When there is no snow on top, this ice is usually blue. Large interconnecting, irregular puddles and a well-developed drainage system are produced during melting.

Figure 2.1 Left: Container ship tracking through a large pan of first-year ice. © Don Isaacs (CIS). Right: Very close pack light nilas and new ice. © C-GCFR (CIS)

Figure 2.2 Top: Frazil ice with fine needles or plates in the water and grease which is frazils coagulated together appearing with a dark, greasy appearance. Bottom: New ice. © [35]

Figure 2.3 Top: Nilas – Less than 10 cm thick elastic crust of ice, which bends on waves. Bottom: Young ice: The gray parts are 10-15 cm thick and are less elastic than nilas. The gray-white parts are 15-30 cm thick and form ridges on its edges from pressure or collisions. © [35]

Figure 2.4 Top: Thin first-year thin ice (30-70 cm). Bottom left: First-year medium ice (70-120 cm). Bottom right: First-year thick ice (> 1.2 m). © Jerry Galt and [35]

Figure 2.5 Old or multi-year ice: Sea ice that has been through at least one melting season.
© [35]

The ice stages of development can be defined as in Table 2.1 [35], [36]:

- Young ice: Approximately 10-30 cm thick. Transition between nilas and first-year ice.
- First-year ice: thicker than new ice (30-200 cm), significant hazard to vessels and ice breakers. First year ice can become impassable when it is deformed into rubble fields and ridges.
- Multi-year ice is generally thicker than 2 m. The internal strength increases, the salinity decreases. The ice is dangerous to ships and off-shore structures.

There are many reasons why it is of interest to have good knowledge about the sea ice, the sea ice thickness, distribution and how it varies inter-annually. There is a lot of undiscovered oil and gas in the Polar Regions (see Figure 2.6), it is important to know about the ice thickness for ice management and new sea routes open up when the ice decreases and covers smaller areas [22]. The sea ice is an important factor for climate change, and hence it is of interest to monitor and understand the Arctic ice and the observed ice decline [1]. Thus, it is important to achieve knowledge of the ice mass balance in the warming environment. Before passive microwave sensors were the main source used to monitor the sea ice extent. But the last years, observations of basin-scale sea ice thickness have been done by satellite altimetry missions to predict the volume of the Arctic sea ice [1].

To be able to compute the ice volume, the ice thickness in addition to the ice concentration is needed. Decrease in ice volume is a factor in the current climate change. Ice thickness is an important factor to know when planning ship and offshore operations. The strength of the ice is correlated with the thickness and the lower and upper surface of the ice are correlated with the thickness.

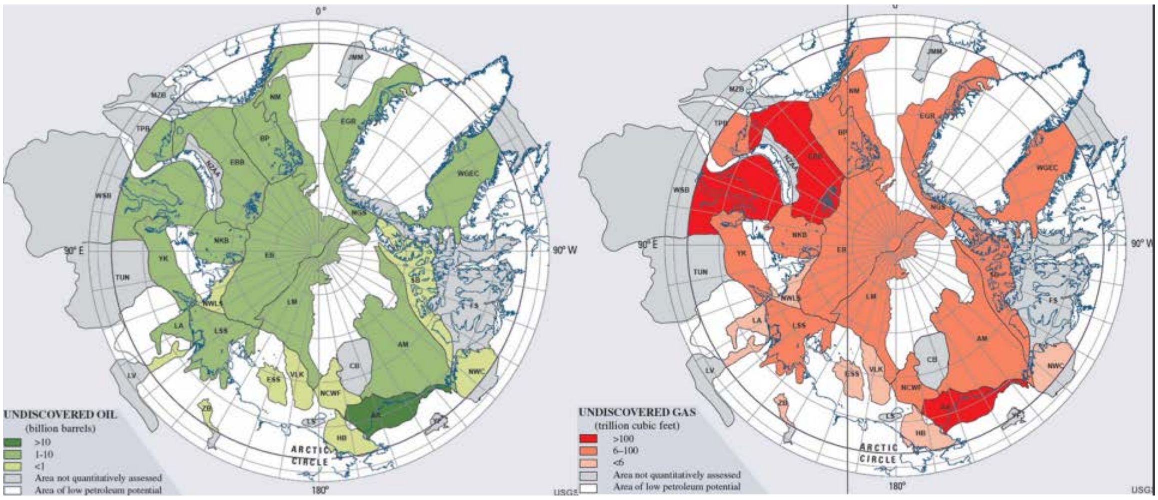

Figure 2.6 Undiscovered oil and gas in the northern hemisphere [22].

The mean thickness of Arctic and Antarctic sea ice is 3 m and 1-1.5 m respectively Sandven [33].

Sandven [34] states that the only way to measure ice thickness thicker than 1 m from satellite is by measuring the sea ice freeboard by radar or laser altimetry. Ricker et al [7] also states that satellite altimetry is the only method where you can monitor sea ice thickness and volume over decades. See more information about altimetry in chapter 4. Other methods must be used to measure the thickness of ice thinner than 1 m. Ice thickness below 0.5 m can be measured using L-band passive microwave data. SAR interferometry can possibly also be used [12]. VIS/IR data can also help giving information about ice thickness with reasonable accuracy (Wang, [39]). Cloud cover, albedo, solar radiation and snow depth affect the results negatively. It is possible to retrieve the mean ice thickness with radar and laser altimetry, but not the maximum ice thickness and ice thickness distribution [12]. VIS/IR data is good for climatological analysis and to see regional and seasonal variations in ice thickness.

Sea ice thickness can be measured with sufficient accuracy now, but the methods are time-consuming or cover small areas:

- Upward looking sonars moored on the ocean-floor (Wadhams [58]) or on a submarine (Wadhams, [68])
- Electromagnetic induction devices on helicopters or ships (Goebell [59], Haas [60], Uto [69])
- Satellite laser altimetry (Kwok, [70])
- In situ measurements (Kwok, [71])

3 Surface and radar reflection

The SAR satellites used for maritime surveillance operate in the microwave region. The Canadian RADARSAT-2 SAR satellite operates in the C-band where the wavelength is 5 cm. Spaceborne SAR gives good possibilities to do effective surveillance of large ocean areas. The RADARSAT-2 ScanSAR Wide mode has a swath width of 500 km, and it takes about a minute to acquire the image.

The radar sends out pulses that reflect off the sea surface. The radar pulses and the objects they hit have different interaction depending on the surface and the incidence angle of the incoming pulse. The factors determining the reflection are [30]:

- The surface's electrical characteristics
- The surface's roughness
- The surface's geometrical structure
- Incidence angle, θ

For liquid sea water the radar pulses are reflected from the top layer. The microwaves at these wavelengths do not penetrate down into the water. If the sea is frozen, the situation is somewhat different. If the ice is dry (i.e. the ice is not in the process of melting) the radar pulses can penetrate a certain distance into the ice, and the backscattering is more complex.

The radar looks down onto the sea surface at an angle, typically with an incidence angle between 20-45º. If the ocean is smooth, the radar pulses will reflect away from the radar antenna, and the reflected signal back to the radar is almost equal to zero. The surface must be rough for the radar to receive any signal back to the antenna of the satellite. The roughness is perceived differently at different radar wavelengths. For a rough surface, the backscattering will go in all directions, thus some of it is going back to the radar antenna. The signal back to the radar is perceived as strong.

On the ocean, the surface waves determine if the surface looks rough for the radar. The reflection mechanisms are complex. The signal strength back to the radar depends on the wind speed, the wind direction in addition to the incidence angle of the radar signal. The water waves are not symmetrical, and thus it is important which direction the radar looks at the waves. Oncoming waves towards the radar give a slighter stronger backscatter signal that the waves moving away from the radar. The weakest reflection is from the waves moving across the radar's direction of bearing [1].

The average radar reflection from the ocean is mostly influenced from waves that have wavelengths that give resonance with the radar's wavelength – so-called Bragg resonance or Bragg scattering. The radar reflection density, σ_0, from the ocean or ice depends on the radar's wavelength, the radar's polarization, incidence angle, the angle between the radar's direction of bearing and the wind direction and the wind strength.

For sea-ice, the surface texture is the main contribution to the SAR image intensity variations. L band SAR has longer wavelength than C and X band, thus making it more sensitive to deformation features like rafting, stamukha and brash [4]. Ice surface wetness also plays a role. Significant melt water on or near the surface results in increased microwave absorption. Multi-frequency SAR observations are therefore particularly useful for discriminating between different sea ice types.

Besides surface roughness and water content, sea ice signatures are determined by the surface temperature, snow depth, internal geometry / microstructure and the salinity of the ice. The last point is not so important, but it might be worth mentioning that the older the ice is, more of the salt is lost, and the electrical properties of the ice changes. The ice will be darker. Some rules of thumb when looking at SAR images with ice:

- Newly frozen ice is relatively dark due to specular reflection off a smooth surface.
- Ice that is being formed in open water will reduce the small ripples, and it looks black in the radar image, as long as the wind is not moderate gale or more wind.
- If there has been a lot of movement in thin ice, it will be divided into small floes with many edges that reflect radar pulses. Likewise the floes can partly be on top of each other, and the surface gets very uneven. This ice will look bright in the image.
- First year ice can vary in brightness due to variation in roughness depending on the amount of ridging and rubbing.
- Multi-year ice is bright because of low salinity and porous structure which gives brighter backscatter [1].

Figure 3.1 shows the scattering mechanisms in ice and snow. The incident wave continuous from air into the snow layer, and the coherent and incoherent fields are scattered by the rough snow-ice-border and also by the ice grains. The part of the wave that comes through to the ice is scattered more by the brine inclusions and by the rough ice-water boundary. Part of the wave is reflected back to the top interface, and is scattered again by the in homogeneities and the rough surface. The multiple scattering can be summarized as the following [25]:

- Surface scattering from below and above the interfaces
- Multiple-volume scattering in the inhomogenous layers
- Higher order interactions between volume and surface scattering mechanisms
- Wave propagation and attenuation in the multilayered anistropic inhomogenous media

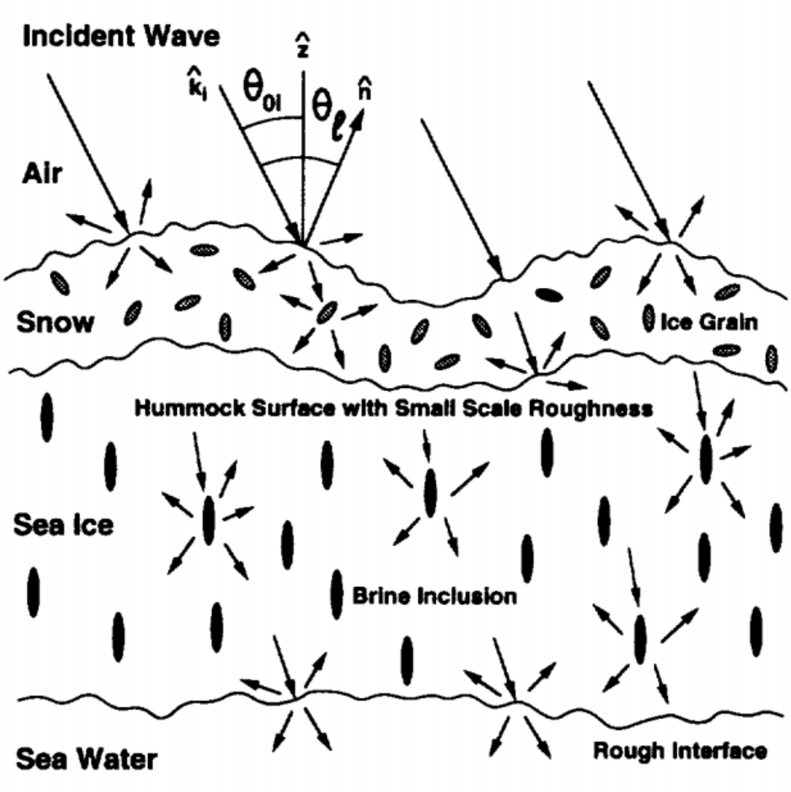

Figure 3.1 The different scattering mechanisms in ice and snow. © [55]

It is almost impossible to operationally monitor sea ice without using data from satellites. By using SAR the sea ice monitoring methods have improved, and can give the following information [34]:

- Ice edge position
- Ice roughness
- Ice concentration/fractional area coverage
- Ice type (new ice, young ice, first-year ice, multi-year ice)
- Ice thickness
- Ice deformation. 50 % of the sea ice is found in areas where there is deformation [34].
- Waves in ice
- Ice drift

Figure 3.2   Ice outside the Oslofjord. What is ice and what is open ocean ? [32]

It is not always so easy to be able to see the difference of what is ice and what is open sea in SAR images. Rough ice will be light, almost independently of the incidence angle. For open sea, the signal will be much stronger for small incidence angles for co-polarization data. Thus, the ocean can be lighter than the ice for small incidence angles and darker than the ice for larger incidence angles. The area in the middle is an area where the contrast between ice and ocean might not be so big. If it is not possible to see if it is water or ice, sea temperature maps can be used from DNMI in Tromsø, Norway or alternatively from US Navy's NAVOCEANO in Stennis. Figure 3.2 shows ice south of the Oslofjord. It is difficult to see what is ice and what is open sea. Figure 3.3 shows drift ice north of Spitsbergen [32]. Figure 3.5 shows rapid ice edge in SAR images due to strong off-ice winds. Other details of the ice are also shown in the figure.

Some examples of explanations of the electrical and scattering properties of sea ice can be found in Drinkwater et al. [105] (1991), Hallikainen and Winebrenner [97] (1992), and Shokr and Sinha [106] (1994), while the electrical and scattering properties of snow are described in Drinkwater and Crocker [107] (1988) and Barber et al. [108] (1998).

Figure 3.3 Drift ice north of Spitsbergen [32].

Ice type charts are created on a near-realtime basis for example by the Canadian Ice Service of Environment Canada (CISEC). Egg codes are used to explain the development stage (thickness), size, and concentration of the ice of both regional and site specific scales. The egg codes conform to the WMO (World Meteorological Organization) standards [31]. Figure 3.4 shows an example of an ice egg. More information about the ice codes can be found on the Canadian Ice Service homepage [109].

The difference between sea ice and freshwater ice can be described as the following. The dielectric constant for freshwater ice varies little with frequency (Hallikainen and Winebrenner [97], 1992). The dielectric constant is given by:

$$e = e' - ie'' \quad (3\text{-}1)$$

e – complex dielectric constant
e' – dielectric constant
e'' – dielectric loss factor

For saline first-year ice, the dielectric constant is higher and strongly dependent on both temperature and salinity of the ice. Only a small amount of brine will alter the dielectric constant of the ice, due to the great value of the complex dielectric constant for salt water. A brine volume of 4% was found to give an apparent dielectric constant of about 4.5. Lower temperature will reduce the dielectric constant. For sea ice, the dielectric constant is relatively constant with frequency above 1 MHz, but the dielectric loss factor is not. There is a minimum in the dielectric loss factor at 3–8 GHz with higher values at lower and higher frequencies. For first-year ice at 10°C and 8‰ salinity, the minimum dielectric loss factor is approximately 0.3. As temperature decreases, the dielectric loss factor increases as precipitated salt goes back into solution; the dielectric loss factor increases with salt content. Multiyear ice has a lower e'' than first-year ice and its temperature dependence is weaker. Thus, microwave radiation penetrates deeper into multiyear than first-year ice. In contrast to water, it is not only the temperature, salinity, incidence angle and polarization that determine the emissivity. The structure of the crystals and of the brine pockets, different for various ice types and ice ages, are also important Sandven [33]. The dielectric constants of the ice surface layers change due to less salt in the ice when the ice grows, and the dielectric constants correlate with the co-polarized ratios and the alpha values.

Deformation of ice due to velocity convergence can change the ice thickness drastically and quickly by local rafting and ridging.

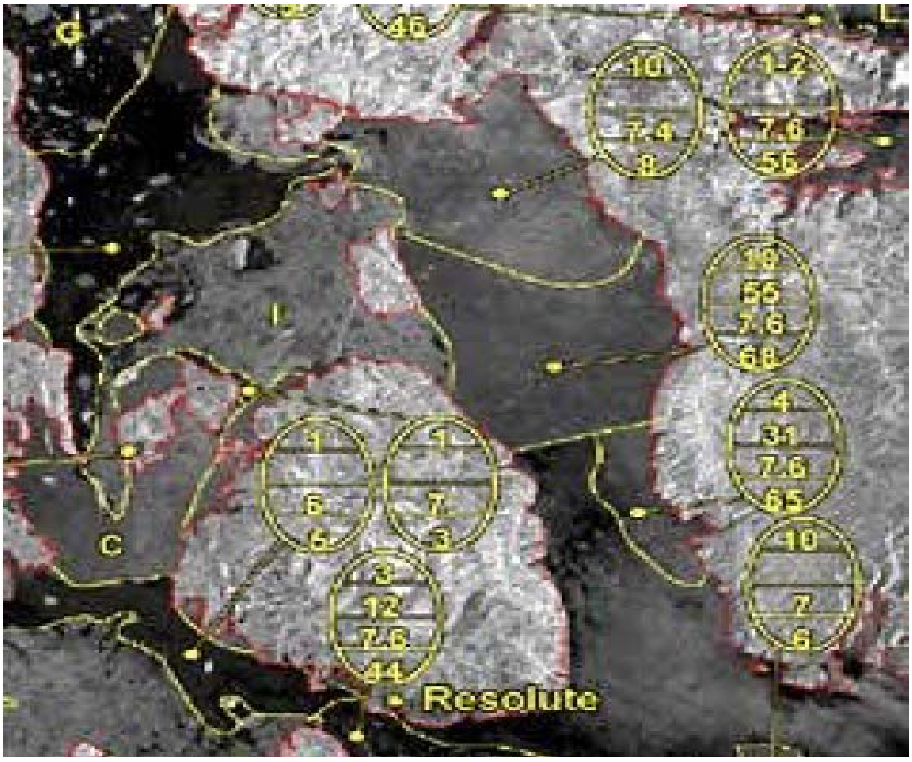

Figure 3.4   Ice egg. © [31]

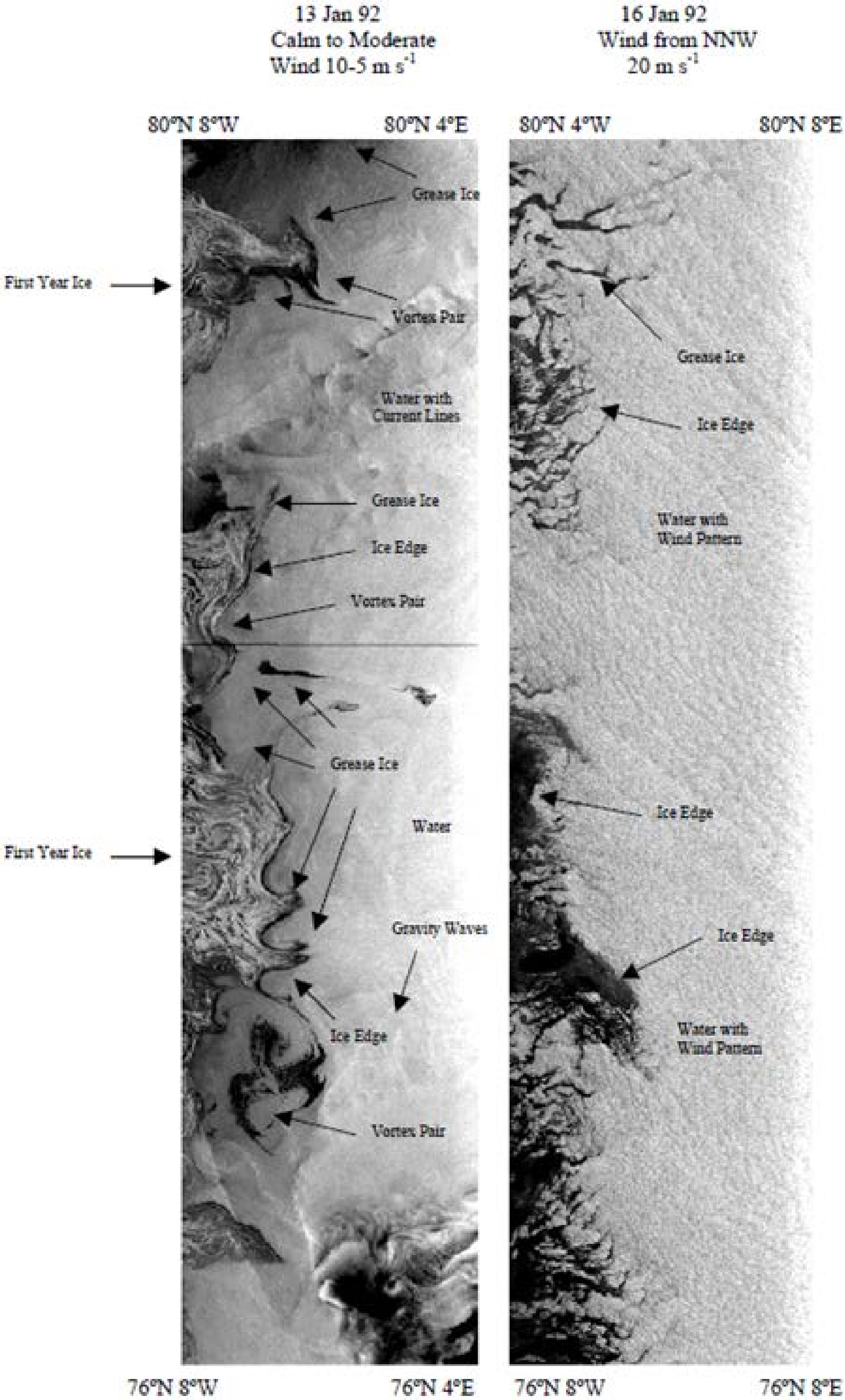

Figure 3.5 ERS-1 images from the Greenland Sea on January 1992 showing rapid ice edge due to strong off-ice winds. ©[110]

4 Ice thickness using altimeter

Altimeters determine the distance from the satellite to the point of interest by measuring the time it takes from the radar pulse leaves the satellite until it returns.

NERSC states in [12] that the only way to measure the thickness of ice thicker than 1 m from satellite is to use radar or laser altimetry to indirectly measure the sea ice freeboard. Spaceborne altimeters on CryoSat-2 and ICESat-2 (launch in 2018) as well as airborne altimeter on IceBridge are now the most accurate way to collect data about ice thickness at high resolution [38]. The altimeters measure the freeboard height below the craft, and it is time-consuming and many days are required to get the ice thickness over a large area of ice. Another disadvantage is that measurements are uncertainties about thickness and density of the snow cover as well as sea ice density. In Antarctica, it is usual with surface flooding since the sea ice freeboard is close to the waterline and due to high snow loading. Laser and radar altimetry measurements differ, and more research is needed on the use of physical assumptions. Ice thickness below 1 m (thin ice) requires additional methods to radar altimetry. Ice thickness below 0.5 m can possibly be measured using passive microwave data. Radar altimetry has the advantage of being able to measure through cloud cover, but laser has the benefit of lack of penetration into snow. It is only possible to retrieve the mean ice thickness with radar and laser altimetry.

Figure 4.1 shows how laser and radar altimeters can be used to measure the sea ice thickness. Laser altimeters measure the snow freeboard, i.e. the sea ice and snow on top, while radar altimeters measure the ice freeboard, i.e. the elevation of the ice, due to different penetration depths of the radar and laser. By assuming hydrostatic equilibrium and using Archimedes' principle, the ice thickness can be derived from the sea ice freeboard.

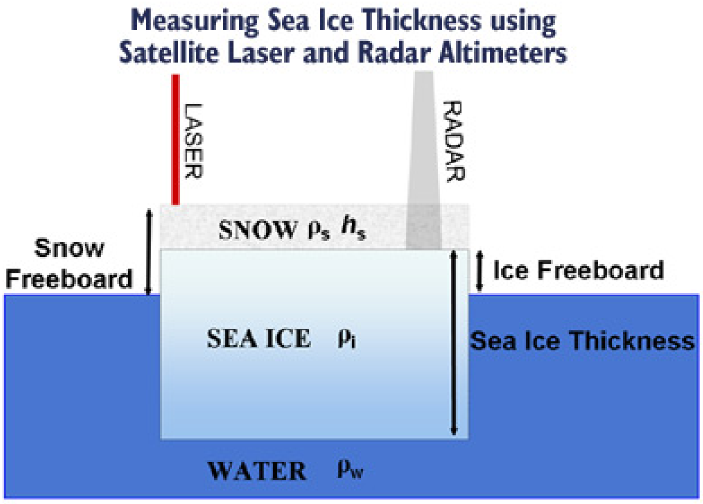

Figure 4.1 Measuring sea ice thickness with laser and radar altimetry © [21]

The freeboard height can be estimated by discriminating between the ice floe and the echo reflections from open water/thin ice, by using special retracking algorithms [13] to find the ice elevations. ERS and ENVISAT have been the primary satellites to measure the inter-annual changes of the sea ice freeboard [13], [14]. Giles et al used a method similar to Laxon et al [13] to estimate the sea ice thickness from freeboard height data with a small additional correction for the travel time of the radar through the snow pack [16]. Here the ice freeboard is defined as the level of the snow/ice interface above the ocean surface [14]. Ice less than 0.5 m thick and open water are not included in the method. The sea ice freeboard height and the sea surface height are measured above a reference height. The return echo shape can be used to discriminate between open water and newly frozen leads and ice floes [17]. The sea surface height is subtracted from the ice freeboard height to give the ice freeboard. By assuming hydrostatic equilibrium, this is then converted to sea ice thickness, using density values of 915.1 kg/m^3 and 1023.8 kg/m^3 for the ice and water respectively [18] as well using snow depth and density climatology [19].

ICESat’s Geoscience Laser Altimeter (GLAS) was the first laser altimetry mission that was able to give large-scale mapping of the ice covered Arctic Ocean, and has been giving data since 2003 [26]. Measurements can be done up to 86°N. The first objective of the mission was to measure changes in elevation of the Antarctic and Greenland ice sheets. Measuring the sea ice thickness is a secondary objective. It is possible to find the mean sea ice thickness, but not the maximum sea ice thickness and the sea ice thickness distribution.

Kwok et al [28] had a first look at ICESat observations of the Arctic sea ice. The sea ice freeboard was measured along the altimeter tracks using sea level references estimated from the thickness of thin ice in recent openings. When converting sea ice freeboard height to ice thickness the unknown snow depth provides the largest uncertainty. ICESat gave a new opportunity to get a view of the Arctic Ocean ice at length scales at and larger than 70 m, which is the altimeter’s footprint. Kwok et al [26] presented a more detailed examination than what was done in [28]. Kwok et al [27] compared ICESat altimeter sea ice freeboard measurements with snow and ice thickness measurements from ice mass balance buoys. The agreement between the measurements is very good. It is found that a time series of ICESat freeboard height can give information about the seasonal changes in snow depth, especially for MY ice. Kwok et al presented results from estimated sea ice thickness in in 10 campaigns done over five years between 2003 and 2008 in [15]. Derived ice drafts are presented and compared with ice draft profiles from moorings as well as from a submarine cruise. The MY ice thicknesses are presented and a net loss is measured in MY ice as well as in the total ice volume and thickness.

Zwally et al [1] also used ICESat to measure the sea ice freeboard relative to an ocean reference level detected over areas of open water/very thin ice. An along-track filtering method was used. The open water/thin ice measurements show good agreement with ENVISAT SAR data. The sea ice thickness is estimated using AMSR-E passive microwave data and nominal densities of snow, water and sea ice.

Renganathan [20] presents in his thesis how the total ice freeboards in the Arctic Ocean were derived from ICESat laser altimetry. The freeboard heights were computed by subtracting the sea surface heights from the measured ice/snow thickness. Geodetic and oceanographic models have been used to model the instantaneous sea surface heights. The Arctic Ocean Tide Inverse Model (AOTIM-5) was used to improve the freeboard estimation accuracy. Good agreements were found when the freeboard measurement results were compared with other methods, for example the “lowest level” method. By assuming a hydrostatic equilibrium, the sea ice thickness in a multi-year ice region was derived from the total ice freeboard. Helicopter-borne Electromagnetic Induction technique was used to compare the thickness measurements. The same procedure as applied in this study can also be applied to other laser and radar altimetry missions, for example Cryosat-2, which was launched in 2010 and ICESat-2, which will be launched in 2017.

Forsberg and Skourup [25] used an improved Arctic geoid model and ICESat laser altimeter measurements to find sea-ice freeboard height using a coarse “lowest-level” surface method. Ground truth data from an airborne lidar underflight shows that the lowest-level method may introduce a bias. Skourup [23] used ICESat laser altimetry data to estimate sea ice freeboard heights as well as gravity anomalies and mean dynamic topography. The “lowest-level” filtering procedure is used to find the sea surface height. Then the sea ice height is found based on this data, and the data showed good correlation with QuickSCAT scatterometer data. If no open water is present, the sea ice height is underestimated. A decrease in the mean sea ice freeboard height is observed from the beginning of the measurements in 2003.

Farrell et al [24] analyzed sea ice freeboard using ICESat. Based on knowledge on the local sea surface height and sea ice elevation the sea ice freeboard is estimated. A time series of data of five years from March 2003 to March 2008 is presented in the article. The results show a decline in ice freeboard height. The decline can be a long-term decrease in ice extent or it may be natural variability. The snow thickness is included in the measurements, and thus it is uncertain if the decrease is only due to ice or if it is variability in snow as well.

Giles et al [5] presents an analysis of data collected during the Laser Radar Altimetry (LaRA) field campaign, which was the first coincident campaign collecting radar and altimetry data over sea ice. The goal of the campaign was to validate ice freeboard satellite measurements, as well as examining the possibility to find the snow depth on sea ice by combining radar and laser measurements. Two methods were developed: 1) a radar retracker and 2) a radar power simulator (models radar returns from the laser data). Elevation estimates from LaRA and ERS-2 radar altimeter over sea ice compare well. No ground truth data were available, but when comparing the difference between the laser and radar reflecting surfaces with snow depth data from climatology there is a consistency.

Following the failed launch of CryoSat-1 in 2005, CryoSat-2 was launched in 2010 and has a Ku band Synthetic Aperture Interferometer Radar Altimeter (SIRAL) onboard where the main objective is to quantify the Arctic ice volume decrease at a global scale [2].

Poulsen et al [29] (2011) used CryoSat-2 data from an area north of Spitsbergen to detect leads in the sea ice. The sea ice is classified from computed freeboard values. The coherence between SAR backscatter and CryoSat-2 altimeter data is evaluated. The surface elevation is extracted and compared with ENVISAT ASAR images. The leads visible in ENVISAT ASAR images and the freeboard heights show strong correspondence.

The conversion from sea ice freeboard height to sea ice thickness is very sensitive to errors in retrieval of the sea ice freeboard and how the input parameters are set for the freeboard-to-thickness conversion. Hendricks et al [1] use CryoSat-2 data to present sea ice freeboard and thickness maps. Airborne validation sets, collected in the international validation program CryoVEx and airborne electromagnetic inductions sounding (spring of 2011 and 2012 and late summer of 2012) are used to check the data. Results from the layout and first results for CryoSat-2 validation campaigns in the southern ocean between June and October 2013 are presented. The data are more uncertain in the Antarctic due to the complicated snow properties. Data is important to analyze since the Antarctic sea ice area is increasing.

Ice extent has shown a decline the last three decades, with a record low in 2012 [6]. Laxon et al uses CryoSat-2 data to test if the decline in ice extent has been accompanied by a decline in ice volume. Estimates for the winters 2010/11 and 2011/12 are done, and the data is validated with in situ data. The results were compared with estimates from PIOMAS and with estimates from ICESat. Between the period from 2003 and 2008 and the 2010-2012 period, the average ice volume declined by 1479 km^3 in winter and by 4291 km^3 in fall. The average ice volume decline is 500 km^3 per year, which is about 7.5 cm decrease in thickness. [6],[8],[9],[10] have all shown that it is possible to see local sea ice thickness features.

Ricker et al [2] used a retracker algorithm and results from airborne validation measurements to evaluate uncertainties of sea-ice freeboard. The main source of freeboard and thickness uncertainty is shown to be from the choice of retracker as well as unknown penetration depth of the radar pulse into the snow layer and surface roughness effects. The freeboard bias is roughly 0.06-0.12 m caused by these uncertainties. Results also showed that it is necessary to use different retracker thresholds depending on the seasonal properties of the snow load.

CryoSat-2 was used over fast ice in McMurdo Sound in Antarctica from 2011 to 2013 to retrieve the sea-ice freeboard. This is the first systematic validation of CryoSat-2 data in Antarctica. Results from a Waveform Fitting (WtF) procedure together with a Threshold-First-Maximum-Retracker-Algorithm at 40 % (TFMRA40) are compared with European Space Agency Level 2 (ESAL2) data [3]. There are errors with the sea surface height identification and radar velocity in snow and a supervised freeboard retrieval procedure is used to reduce the errors. The ESAL2 sea ice freeboards are overestimated, while WtF is within 0.04 m of the ice freeboard. Due to variable snow conditions and other uncertainties, the estimated height is 0.14 m over the observed ice freeboard. TFMRA40 freeboards are at the most only 0.03 m away from the snow freeboard. The different assumptions of each retracker give the separation of the freeboard estimates. The article presents automatic freeboard retrieval procedures for ESAL2, WtF and TFMRA40. Freeboard data from CryoSAT-2 found by using all three automatic procedures are in line with well-known sea ice growth rates in Antarctica.

Armitage et al [4] addresses the problem of the uncertainty associated with the knowledge of the snow layer depth and how the radar interacts with the snow when retrieving sea ice thickness.

They have done a comparison between CryoSAT-2 data and data from AltiKa Ka band radar altimeter during one season of ice growth between 2013—14. CryoSat-2 measures freeboards that are 4.4 cm and 6.9 cm smaller in October 2013 and March 2014, respectively. Airborne laser and radar measurements are used to find the effective scattering horizon for both CryoSat-2 and AltiKa.

The only way to monitor the sea ice thickness and volume changes over time is by using altimetry data. Altimetry missions are for example ERS, ENVISAT, ICESat and CryoSat-2. The freeboard is converted into thickness by assuming hydrostatic equilibrium. Ricker et al [7] investigates the impact of geophysical range corrections on sea ice freeboard. The impact depends on the interpolation between subsequent leads when retrieving the sea surface height as well as the magnitude of the correction. The impact is investigated by looking at freeboard in autumn and spring. The conclusion from the study is that the most parts of Arctic are not affected much by the corrections. The impact can be substantial in areas with very low lead density, for example where there is multiyear ice (north of Canada) and landfast ice zones.

Snow cover on ice has a lot of influence on the properties of the underlying ice, the growth/melt rates, the size and formation of melt pounds and the albedo [38]. Satellite altimeter measures the ice freeboard line when calculating the ice thickness, and snow cover can make the measurements from satellite altimeter data inaccurate. The snow cover depth and density are very different between Arctic and Antarctic sea ice. Heavy, wet and saline snow is very common in the Antarctic, as well as in the Sea of Okhotsk, while in Arctic the snow is more dry and transparent to the radar. The wet snow in the Antarctic can lower the ice level below the sea level making a mixture of slush and re-frozen ice layers around the sea ice and snow border. This is difficult to handle in models.

Some success measuring snow depth on sea ice has been made by using PMR data [48], but there are some limitations due to melt conditions and rough ice [49]. Techniques using PMR data have also been used to estimate snow thickness in [16], but are limited to snow depths less than 50 cm, are not accurate for MYI, and have inaccuracies due to atmospheric effects and repeated freeze/thaw cycles [47]. Snow depth on sea ice data has been collected by NASA since 2006 using airborne altimeters and Advanced Microwave Scanning Radiometer for Earth Observing System (AMSR-E) simulator. There are still knowledge gaps of the impacts of the snow cover on the sea ice and of the overall thickness distribution across both polar regions [38]. Using multi-frequency, multi-polarization SAR data to estimate the snow depth on sea ice, among other properties, has been investigated in [51].

The ongoing study CORESAT (Combined remote sensing and in situ study of sea ice thickness and motion in the Fram Strait) at Nansen Environemental and Remote Sensing Center has a primary objective to get a better understanding of how to use satellite remote sensing to the sea ice thickness and drift distribution in the Fram Strait [117]. The Fram Strait is the main gateway where the sea ice exits the Arctic Basin. Another objective is to obtain a longer dataset with higher temporal resolution, than earlier datasets, over the ice in the Fram Strait. Reliable error margins will be established and satellite date from different seasons over multiple years will be validated with in situ data. The study will obtain a sea ice volume export estimate. Satellite data from ICESat, low-resolution radiometer/scatterometer, CryoSat-2, SAR satellites and SMOS will be used in the study and the results will be compared with in situ measurements from ship, ice station and helicopter. ICESat and CryoSat-2 will be used to obtain sea ice freeboard/thickness, SAR will be used to look at sea ice drift while SMOS will be used to estimate thin ice thickness.

5 Ice thickness using SAR

It is important to know the ice thickness for operational purposes and to able to understand the dynamics and the thermodynamics in the Arctic and Antarctic. SAR can provide all-weather and all-day (independent of solar illumination) capability at high spatial resolution and is good for mapping in general. SAR gives relatively frequent coverage and acceptable resolution.

The surface texture can give information that can be used to find ice age and ice thickness. SAR images can give information about ice types which can give an approximate estimate of ice thickness. Automating the segmentation and/or the classification process saves much time and also the insecurity of the varying skills of the analysts. Figure 5.1 shows an example of classification of ice types using SAR [34].

Somewhat steeper incidence angles, down to 10 or 15 degrees than what exist on the common SAR satellites today may be proven to be advantageous. This requires at low noise floor (-35 dB), to minimize the noise at higher incidence angles from low backscatter returns such as smooth ice [38].

The repeat frequency of observations can be lower in the middle of a stable ice pack, but in the marginal ice zone, more frequent observations are required, at least daily observations. The spatial resolution for climate models of 10’s of kilometres is sufficient. A resolution of 10’s of metres on a daily basis is needed. Spatial resolution of meters and temporal frequency of hours are required for tactical support for ships and offshore structures [38].

ICESat, CryoSat-2, TerraSAR-X, Cosmo SkyMed and RADARSAT-2 are sensors now used to give information about ice thickness. IceSat-2 and Sentinel-3 are future satellites that will give information about ice thickness.

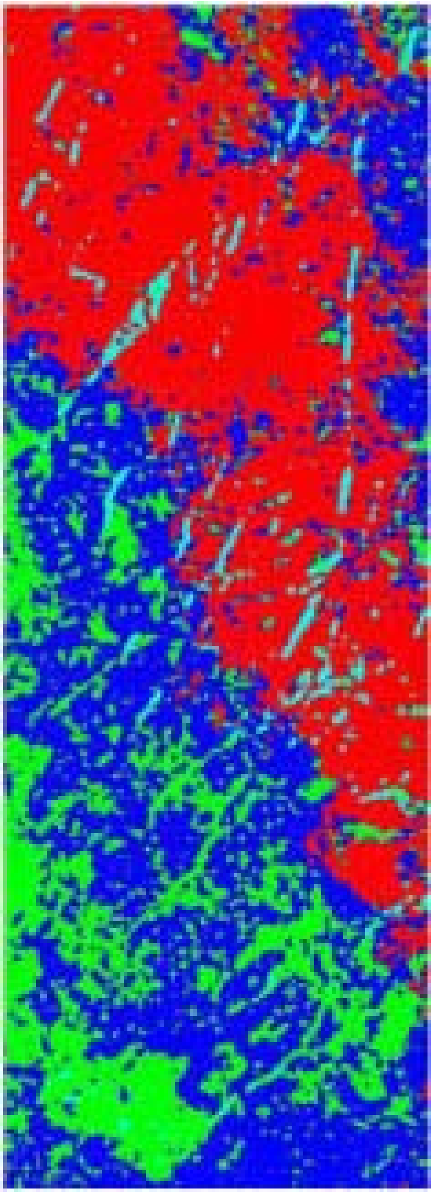

Figure 5.1 An example of an image showing classification of ice types: 1) Undeformed first-year ice (green), 2) Deformed first-year ice (dark blue), 3) Multi-year ice (red), and 4) Open water or thin ice (light blue) [34].

5.1 Ice thickness and polarization

Polarimetric SAR data have the potential of estimating the ice thickness. Polarization is an important factor when working with sea ice detection using SAR images. Ice, snow, water and the boundaries between these, have different scattering properties in the different polarizations and polarization combinations that are available on the SAR satellites in orbit today. How the radar signal is reflected back to the satellite depends on the roughness of the ice surface, snow cover, water content in the ice and snow, ice salinity, and the motion of the ice. Depending on the complexity of the sea ice, the number of reflections from the sea ice can be even (double) and odd (single and triple).

Using more polarization channels gives more information about the ice [67]. The major limitation of dual- and quad-pol SAR data is the limited swath width. New possibilities open up with compact polarimetry (CP) data since they have more polarization information than dual-polarization data has and they have much greater swath widths than the quad-polarization modes have [65]. One disadvantage of CP data is that it is not possible to retrieve the co-polarized and the cross-polarized ratios directly.

Many researchers are sceptical about using information only from SAR data to do ice thickness estimation [113]. Kwok states that he doesn't have any experience of retrieving ice thickness from SAR images using only backscatter. HV-polarization is good to use to distinguish highly smooth surfaces from rough surfaces when the co-polarization ratios (VV/HH) are not available. Co-polarization SAR images can be used "as proxies of thickness" [111], but the resolution is coarse.

5.2 Ice thickness using dual-polarized data

To do ice classification operationally, dual-polarization has become the standard mode, either HH + HV or HH + VV (Falkingham, [8]). Using the RADARSAT-2 ScanSAR Wide mode, every location north of 65 °N can be imaged at least once every day [37]. [8] states that using multi-frequency and multi-polarization SAR data with increased repeat frequency in addition to other sensors like VIS/IR, PMR, AMS and altimeters can be used to get more accurate ice thickness fields. More research needs to be done to understand how the radar waves reflect off of the complex sea ice. Sea ice thickness is the most important parameter to understand better. It is also important to get an overview of the snow cover distribution.

Estimating ice thickness with SAR for flat, thin ice (< 30 cm) has been demonstrated with some success by Kim et al. [41] and Zhang et al. [42]. Kim et al. [41] used RADARSAT-2 and TerraSAR-X SAR data to estimate sea ice thickness by looking at the relationship between the co- and the cross-polarized ratio to measure the degree of depolarization effects in estimating sea ice thickness for thicker ice, thick FYI and MYI in the Arctic Sea (summer time). Thicker/older ice is rougher and less saline. For MYI, the salinity decreases, the complex dielectric constants decrease, the penetration depth of the radar wave increases, and the volume scattering increases. The degree of depolarization is linked to the thickness of the older ice as ice surface roughness increases and salinity decreases. There is a strong correlation between the sea ice thickness and the depolarization factors, i.e. co-polarized correlation (VV & HH) and cross-polarized ratio (HV/HH & VH/VV). Multiple scattering from snow/ice interface and volume scattering increase the depolarization effects for those ice types, and the depolarization of the radar return signals are higher. Kim et al used a combination of numerical modeling works, in situ sea ice observations and polarimetric SAR data. There might be a viable thickness-to-depolarization relationship, especially for the deformed ice case. In situ measurements were done by a snow probe and electromagnetic induction system. The low salinity of MYI upper layer makes it possible to discriminate between MYI and FYI during winter. This is not possible during melt season due to the wet snow and water on top of the ice, Sandven [33], 2006. Another phenomenon of importance for remote sensing during winter is the formation of frost-flowers in cold weather on top of thin, high saline ice. These crystals, which have dimensions of a few cm, cause very high backscatter of the radar signal.

Backscattering values simulated by Fung and Eom [75] can be used to find the degree of depolarization due to volume scattering. Zhang et al. [42] combined a multi-layered sea ice electromagnetic scattering model with a sea ice thermodynamic model to assess the determination of the thickness of flat thin ice (<30 cm) in the Bohai Sea using SAR at different incidence angles, frequencies, and polarizations. Co-polarization backscattering coefficients and the co-polarized ratio can be used for C- and X-band SAR, while the co-polarized correlation coefficient can be used for L-, C-, and X-band SAR. Low or moderate incidence angles should be used to avoid the effect of speckle noise. When the salinity of sea ice decreases, the complex dielectric constant decreases. When the ice dielectric constant decreases, the CPR (co-pol ratio VV/HH) and ρ decrease, so the CPR and ρ are negatively correlated with ice thickness. With the decrease of the complex dielectric constant for sea ice and the increase of surface roughness, the surface scattering and volume scattering is enhanced and as a result the total backscattering signatures increase.

It is shown that L-band in combination with C- or X-band is the most promising. S-band SAR should also be investigated further (Falkingham [38]).

SAR data may not be good to monitor interannual changes in ice thickness, especially for thick ice, since it only measures the ice thickness indirectly by measuring the roughness of the surface due to rough ridged ice and old ice which has a lot of air pockets and low salinity. Flooding and snow cover might hide the ice thickness information Wadhams [79], 1992. Wadhams et al [78], 2004 used a new wave dispersion theory to measure thickness from SAR imagery in Antarctic pancake ice.

Leigh et al [80], 2014 presents an automated ice-water classification system, Map-Guided Ice Classification (MAGIC), using dual-polarization RADARSAT-2 images. The method shows promising results and is under consideration of the Canadian Ice Service for operational use. (Only to classify ice/water)

Haverkamp et al [90] tested 90 ERS-1 SAR images and classified them into <30 cm, 30-200 cm and 200 cm using a local thresholding technique. The use of a local dynamic thresholding technique preserves the local contrast in the original SAR image. The method showed good separation among ice thickness classes. Ice growth and behavior, geographical, and historical knowledge can be used to supplement the original classification to get the proper labelings for the ice thickness classes. In situ verifications were not done, so only visual inspections of the classification maps were done.

Estimating ice thickness using the co-polarized correlation coefficient with a ship-based C-band radar system for flat, newly formed thin FYI (< 69 cm) has also been demonstrated with some success by Isleifson et al [93]. Two ice thickness regimes were suggested, less than 6 cm and more than 8 cm, due to the difference in surface roughness and/or brine cells between. They found a relationship between the depolarization factors and thickness. Physical data from 40 stations were used as ground truth.

The observed increase in the backscattering coefficient during early sea ice growth and changes in sea ice properties linked with growing thickness (e.g., vertical dielectric profile and size of brine inclusions) may explain such correlations. The difference between radar intensities at VV- and HH-polarization is relatively sensitive to the dielectric constant of the near-surface ice layer, which is, in turn, related to ice thickness via corresponding changes in near-surface ice salinity. In one study from the Antarctic, even ice thicknesses up to about 1.2 m could be retrieved with reasonable accuracy based on the co-polarization ratio at C-band [40]. Correlations between ice thickness and radar signatures are similar at L- and C-band. Because the L-band radar signature is often less affected by the small-scale roughness of the ice surface but is more strongly influenced by deeper portions of the ice, its use may offer an advantage. On the other hand, the scattering intensity from thin ice is lower and hence closer to (or even below) the noise level at L-band. In one direct comparison, L-band radar was less sensitive to ice thickness compared to C-band [71]. It has also to be emphasized that “disturbing” factors such as frost flowers or rafting processes that influence the radar signature have to be taken into account and may overlay the effect of ice growth. Correlations were also found for thicker ice classes, even when using only radar intensity. In this special case, it was speculated that surface roughness, at both small and large scales, was changing with ice age.

Kwok [77] described an analysis technique for thin ice distribution (< 2 m) in the Arctic Ocean. Ice age and thickness are estimated from repeated observations of Lagrangian elements or cells of sea ice in sequential SAR imagery. Ice age is converted to thickness using an empirical ice growth formula. The technique works only during winter ice growth season. The maximum likelihood classifier and lookup table of expected backscatter [71] are used to classify ice into FYI or MYI. Kwok et al [43] execute a Lagrangian analysis of sea ice motion, which is coupled with a thermodynamic model. This method can be used in Arctic and Antarctic to estimate ice thickness distributions. This technique has been tested and demonstrated in the Gulf of St Lawrence on a smaller scale by Karvonen et al [44]. At least daily repeat frequency is required in Lagrangian analysis, which is a challenge especially in the Antarctic [38].

C-band ScanSAR Wide Swath SAR data from ENVISAT and RADARSAT-1 were used by Similä [86] to estimate sea ice thickness under 50 cm. The SAR image was first segmented, and then the ice thickness distribution is assigned to each segment. Ground truth data used was helicopter-borne electromagnetic induction sensor (EM) in the Baltic Sea. The results showed a strong correlation between the ice thickness and the backscattering coefficient σ^0. HH and VV SAR data were used. The values measured over rough level ice and ridged ice fields overlap each other significantly [87], so the σ^0 values are ambiguous. It may be possible to use this proposed method on Arctic areas according to results presented by Prinsenberg [88], where

ENVISAT ASAR data was used on first year land-fast ice and mobile pack ice. The next step is to study the conditional ice thickness distributions given the ice type.

Winebrener et al [98] reported that the VV-to-HH polarization ratio and the phase difference between HH and VV were related to ice thickness, especially for thin ice in Antarctic leads. A relationship between young ice thickness and backscatter is shown by Zabel [72] and Matsuoka [73]. The VV/HH ratio was shown to respond to salinity in the ice during the Coordinated Eastern Arctic Experiment´89 [74].

Good correlation between thin ice thickness and BCRs (Backscattering Coefficient Ratio) retrieved from polarimetric SAR data were showed by Wakabayashi [61], Nakamura [62], Nakamura [76], and Nakamura [40]. The results are applicable for newly formed thin ice using dual-polarization data.

Wakabayashi et al [61] used L-band airborne SAR data to investigate SAR data before launch of ALOS. Airborne quad-polarimetric and interferometric Pi-SAR data in the Sea of Okhotsk were used. The low depolarization characteristics of open water could be used to discriminate it from sea ice by scattering entropy in all incidence angle ranges. From the relation between ice thickness and the polarimetric parameters, they found that backscattering coefficients and VV/HH backscattering ratio are highly correlated with ice thickness. Since the ratio is sensitive to ice surface dielectric constants, a simple simulation using the integral equation method surface model was conducted by using the physical parameters of typical sea ice. A two-dimensional ice thickness map was derived from an empirical relation between the VV-to-HH backscattering ratio and ice thickness. Ground truth data is a mooring buoy system.

Nakamura [62] proposes a polarimetric decomposition technique to classify sea ice. Sea-ice thickness is estimated based on multi-polarization (HH and VV) and dual-frequency (L- and X-band) SAR-data. The VV/HH backscattering ratio is used to estimate the sea ice thickness, since it has little sensitivity to the ice surface roughness, but may reflect differences in the ice-surface dielectric constant and thus the thickness. The Airborne Pi-SAR (polarimetric and interferometric) data is used as ground-truth. The sea ice types were divided into three simple types, New Ice (less than 10 cm), Young Ice (10-30 cm), and First-Year Ice (30 – 120 cm). The method is generally applicable to sea ice during ice-growth season.

Nakamura [76] used C-band ENVISAT and L-band Pi-SAR data to measure the sea ice thickness of undeformed FYI. The use of L-band provides almost a factor of 2 of improvement in accuracy over the C-band. The correlation between VV/HH-ratio and sea ice thickness is larger than the correlation between the backscattering coefficients and the sea ice thickness. This is because the ice surface salinity and hence the surface reflection coefficient decreases as the ice thickens. Developed algorithm for retrieving ice thickness based on the backscattering ratio and on the integral-equation-method (IEM) surface scattering model. The algorithm performed better than previous retrievals using an empirical technique.

Nakamura [40] used ENVISAT ASAR dual-polarization data from Lützow-Holm Bay in East Antarctica for estimation of sea ice thickness. In-situ measurements of the ice thickness were compared with the reflection coefficients for each polarization (HH, VV, HV, and VH) and the VV/HH ratio. It was shown that it is possible to use the VV/HH backscattering ratio and the backscattering coefficients for each polarization to get a good estimation of the sea ice thickness. The VV/HH ratio depends on the near-surface dielectric constant of the sea ice, and this constant is related to the developing process of the ice and the near-surface sea-ice salinity, and thus the ice thickness. Based on in-situ observations there is close first-year pack ice and fast ice in the test area. Since the ice is relatively old, the VV/HH ratio is expected to depend on changes in the near-surface dielectric constant caused by salinity-driven changes, and not by changes in the surface roughness. The results are based on the empirical relationships between ice thickness and the VV/HH backscattering ratio with linear and logarithm fits. The linear fit is recommended for fast ice, and the results showed an rms error of 0.08 m and a correlation coefficient of 0.91, and thus provides a reliable result.

Geldsetzer and Yackel [52] 2009 used dual-polarized C-band ENVISAT ASAR APM imagery to investigate the ability to discriminate sea ice types (thin ice, FYI and MYI) and open water during winter based on backscatter magnitudes (VV and HH) and polarization differences (VV/HH ratio). Visual discrimination is enhanced using colour composite imagery (VV, HH, VV/HH) and Gaussian stretch. The smoothness of the ice surface can be inferred from dual-pol imagery. It is difficult to discriminate water and thin sea ice using only single- or dual-polarized SAR imagery, especially for small incidence angles. Ground truth data used is ice charts from CIS (Canadian Ice Service).

When sea ice is deformed, the surface roughness is increased due to compression processes. Ridging and rafting (deformed ice) affect the large-scale surface roughness, and thus this can be used to estimate the ice thickness according to Peterson et al [66] and Toyota et al [63]. Peterson et al measured FYI surface roughness and ice thickness using a fix-mounted helicopter-borne electromagnetic (HEM) laser system in Amundsen Gulf (Arctic) in 2004. These data were compared with ENVISAT ASAR AP and RADARSAT-1 data. Roughness properties as proxies may be used to estimate the thickness distribution of sea ice. Toyota et al [63] showed that there is good correlation between large-scale surface roughness and sea ice thickness for thicker ice due to ridging and rafting processes. L-band backscattering data in the southern Sea of Okhotsk in 2005 are used. In situ measurements were done with ship-borne EM induction sensor and supersonic profiling of sea ice thickness and surface roughness. Ice thickness between 0.44 and 1.65 m can be estimated from L-band radar backscattering coefficient with the rms error of 0.19 m. They used HH, VV and co-polarized ratio (VV/HH) to analyse the data.

Karvonen et al states that it is practically impossible to estimate ice thickness from RADARSAT-1 SAR images alone [89], because the surface scattering dominates the backscattering at C-band [101]. They introduced an algorithm for sea ice thickness estimation by augmenting the sea ice thickness history derived from daily digitized ice charts for the Baltic Sea ice. The algorithm is designed for operational use and produces ice charts based on several different data sources, for example C-band RADARSAT-1 ScanSAR Wide mode HH data with 100 m resolution as well as field observations. An estimated minimum, mean and maximum ice thickness values are assigned to each segment based on the digital ice charts. The goal is to get a more accurate ice thickness estimate than the relatively coarse ice thickness information the ice chart gives. The SAR data are processed to a logarithmic intensity scale, sent to FIMR, rectified to Mercator projection and land areas are masked off. The incidence angles must be corrected for in the SAR images and an incidence angle normalization algorithm for Baltic Sea ice is used [102]. A slightly modified isodata clustering algorithm is used to segment the image [103].

Karvonen et al used ScanSAR RADARSAT-1 HH and RADARSAT-2 HH/HV images to analyze ice thickness distribution in the Gulf of St. Lawrence off Canada, and presented the results in 2012 [44]. A novel automated method for deriving ice concentration and thickness was presented, and the results were promising. The method is based on input data from a high-resolution thermodynamic snow and ice model (HIGHTSI), SAR-based ice motion, and SAR texture features and produces ice concentration and thickness estimations. Multiple SAR images over the same area with reasonable temporal difference will improve the ice thickness estimates by using a temporal minimum. The results were validated using local EM measurements over a short temporal period and (Canadian Ice Service) CIS ice charts. The method is more detailed and physical information on spatial distribution of the ice thickness, than the operational method being used at the time (visual interpretation of SAR data). The method has potential for operational use and is applicable in all seas. In-situ data throughout a complete season is needed to calibrate and validate. Comparisons have been made CIS ice charts and EM data.

There are some challenges in estimating ice thickness using SAR. One is to locate areas of thin ice. SAR backscattering and texture for deformed thin ice is sometimes very similar to the values for deformed thick ice areas. It has been shown that using radiometer data (to estimate the thickness of thin ice [94], [96], [95] together with SAR data is useful for better estimation of overall ice thickness according to Karvonen [82]. Only HH-polarization data was used, and tests/study on dual-polarization data was proposed. Development and evaluation of dual-polarized data will require data from at least one complete ice season. A more advanced method for ice concentration estimation than the one described in [44] is presented in [82]. The test data set used is RADARSAT-2 HH-polarized ScanSAR Wide mode data. Ice concentration estimates at high resolution (500 m) are based on C-band SAR data and on segment-wise autocorrelation distributions. Ground truth data is Finnish Ice Service (FIS= ice charts and ice concentrations from the radiometer-based operational ice concentration algorithm of University of Bremen. The SAR ice thickness algorithm estimates the ice thickness using the modelled ice thickness distribution, kinematic features based on the SAR ice drift, SAR features, and SAR ice concentration as inputs. The ice thickness algorithm utilizes the SAR features, ice thickness modelled by High-Resolution Thermodynamic Snow and Ice Model (HIGHTSI), kinematic ice features (DT, RM) derived from the SAR-based ice drift, and ice concentration from the SAR ice concentration algorithm. The incidence angle is corrected for and mapped to 30 degrees by using a linear dependence for the logarithmic σ^0 values [102].

Karvonen is now working on using dual-polarization data to do ice thickness estimation [112]. Using dual-polarization data, HH/HV, improves the ice thickness estimation compared with using HH-polarization alone. He states that SAR alone cannot be used to do sea ice thickness estimation, even though dual-polarization data are available. Some background information is needed, for example an ice model or some other Earth Observation instrument that can produce rough scale ice thickness estimates. This can be retrieved from SMOS or altimeter. If it is possible to use radiometer data to locate thin ice areas, the results are further improved. Doing sea ice thickness estimation using dual-polarization data alone may work for some areas, but well-calibrated SAR backscattering is needed and different temperature conditions and incidence angles must be taken into account. Using only SAR to do sea ice thickness estimation can work in cold weather for a certain area. For another sea area, a different parameterization is needed, thus making it tricky [112].

Fors et al [81] investigated five polarimetric properties and their relationship with sea ice thickness in late summer sea ice. Cross-polarization ratio is a measure of depolarization, and indirectly sea ice thickness. Differences in depolarization are due to difference in surface roughness between young (thin ice) and older (thicker) ice, as well as sea ice structure differences (grain size and size and amount of air pockets). The salinity of the end of FYI and MYI is expected to be similar due to most of the brine inclusions are being flushed away during the melt season. The relationship between the cross-polarization ratio and the sea ice thickness is possibly dependent on incidence angle. More research needs to be done. The strongest correlation is obtained with high incidence angles. Sea ice thickness measurements are dependent on location of ice, the time of year and the growth history of ice.

5.3 Ice thickness using quad-polarized data

Based on previous research Zhang et al [57] expect a potential to use compact polarimetric C-band SAR data under certain conditions for thickness retrieval of undeformed first-year sea ice. The compact data is made from RADARSAT-2 quad-pol images. A parameter is used which is called the CP-ratio, and the ratio’s sensitivity to the dielectric constant, thickness, surface roughness, and incidence angle is investigated.

The CP-ratio is given by:

$$CP - ratio = \frac{\langle |R_S - R_P|^2 \rangle_{|\theta_l}}{\langle |R_S + R_P|^2 \rangle_{|\theta_l}} \tag{5-1}$$

Her R_S and R_P are the Bragg scattering coefficients perpendicular and parallel to the incident plane. θ_l is the local incidence angle. Optimal conditions for the thickness retrieval are deduced. RADARSAT-2 quad-pol data are used to generate C-band CTLR (Circular Transmission and H and V receptions) SAR data, and are compared to helicopter-borne sea ice thickness measurements in the Sea of Labrador. Empirical equations to calculate the thickness are tested. The most promising result is an exponential fit between the CP-ratio and ice thickness, H. More research needs to be done in the future. The CP-ratio is given by:

$$\text{CP-Ratio} = 0.2014 - 0.06383 \cdot \ln(H) \tag{5-2}$$

Compact polarimetry data are very useful to estimate the thickness of first-year ice thickness. The thickness distributions can be obtained at a much higher spatial resolution than earlier results using SMOS (Soil Moisture and Ocean Salinity Mission). The thickness of deformed thicker ice was not studied due to lack of ground true data to compare with, since the thickness often is underestimated by the EMS measurements by as much as 50 or 60 %.

Fully polarimetric SAR data has too limited coverage to do fully ice thickness mapping of an area, but it can be useful to monitor small local areas [8]. It can also be used for research of how the physical processes are when radar waves interact with the sea ice of varying thickness. Table 5.1 shows the observation requirements necessary to be able to estimate sea ice thickness [8].

Using quad-polarimetric SAR data can help classifying different ice types with improved accuracy. An automated algorithm was compared to analysis by manual analysts in [56]. The algorithm classifies the ice into a specified number of classes by analyses of the statistical and polarimetric properties of the backscattered radar signal. More research needs to be done to be able to know how weather and viewing geometry alter the backscattering signal. The SAR scene is divided into five classes and by the automated algorithm, while the SAR experts were able to distinguish between three classes in optical images. By doing physical interpretation of the polarimetric parameters, two more ice classes were able to be labelled in terms of deformation level. The RK parameter, not previously used for ice segmentation, helps to distinguish between deformed and smooth ice. Polarimetric SAR data will increase the efficiency and exactness of ice maps.

Table 5.1 Observation requirements to be able to estimate sea ice thickness. © [8]

Target Geographic Location	• Global polar and sub-polar sea ice areas • Arctic Ocean ice export gateways (Fram Strait, Kane Basin, Northwest Passage) • Antarctic regions around bases and experimental sites
Repeat Cycle	• At least daily • Every 6 hours in cases to capture diurnal and tidal effects
Resolution	• 10's of km for climate models • 10's of m for NWP • <10m for tactical support and process research
Frequency	• C+L or X+L • Investigate S
Polarization	• Multi-polarization (HH, VV, HV, VH) • Research with full polarimetry
Incidence Angle	• 10-50°
Seasonality	• Year-round
Complementary Sensors	• Altimeters, Low frequency PMR, VIS/IR

Lang et al showed in [53] that estimating ice thickness can be done with single pass interferometry, for example with TerraSAR-X/TanDEM-X. The technique works best for incidence angles below 30° and with interferometric baselines of more than 300 meters. Doing more research on this topic, both on single-pass and repeat-pass (no more than a few days) modes, together with obtaining altimeter data, to obtain the sea level reference is of interest.

The possibilities of combining high resolution SAR together with VIS/IR, or other Earth observation instruments as PMR and AMS, are of great interest due to the wide coverage that SAR offers.

It is of interest to combine L-band with either C-band or X-band. Observations from all SAR frequencies would be of interest to get the most information about ice thickness. Further research on the use of compact polarimetry is needed. The resolution should be between 10 and 100 m and the repletion frequency should be as low as possible.

Systematically monitoring the three high priority variables, sea ice thickness, snow cover and sea ice deformation, with space-borne SAR has been of little success [38]. But a breakthrough is expected by using some combination of polarization, frequency and incidence angles.

Moen et al has explored physical properties of sea ice, such as thickness, in fully-polarimetric SAR data in [54] using several steps. A classification algorithm, using both polarimetric and statistical modelling, is first used to segment the SAR image into distinct classes. Then the segments are analysed by sea ice experts and scattering properties from polarimetric analysis are provided. The sea ice is classified into sea ice types and estimation of sea ice geophysical properties is done in the end.

6 Operational estimation of ice thickness

This chapter gives some examples on how different ice centers or meteorological institutes do sea ice thickness estimation operationally.

The U.S. National Ice Center use SAR data in their analysis when doing ice thickness estimation, but they do not base the thickness of the ice on SAR data. The sea ice thickness is estimated based on knowledge of the age and characteristics of the ice, according to World Meteorological Standards. The U.S. National Ice Center does many different types of analyses. Daily they produce a hemispheric analysis of the marginal ice zone and weekly they produce a detailed hemispheric analysis of sea ice types and concentrations [115].

The Finnish Meteorological Institute does research using dual-pol SAR data for sea ice thickness estimation. Tests have been done to operationally use and produce ice charts based on several different data sources. One of the data sources have been SAR HH-polarization images. The newest research of Karvonen et al has not been published yet, because it is still ongoing work, but using a combination of HH and HV improves the sea ice thickness estimation compared to using HH alone [112].

Many different data sources (SAR and optical imagery, ship reports and aircraft reports) are used by the Canadian Ice Service to produce ice charts manually. The analysts' knowledge of the ice and associated environmental conditions are used to give an estimation of ice concentration and stage of development. The ice thickness is given in ranges using centimetres. For example new ice is between 0-9 cm thick. SAR can be used to see what stage the ice is in, because the SAR backscattering changes as the ice thickens [114].

The Ice Service in Norway is part of Norway Coastal Administration's service. It provides ice condition information, and does mainly two tasks:

1. Updated information about ice conditions in Norwegian waters from the Swedish border to Kristiansand.

2. Do icebreaking outside harbours in primary and secondary fairways. Ice reports are updated at kystverket.no during the months of December through March.

Each business day ice maps are created over the Norwegian part of the Arctic, as well as other parts if necessary, for example the Oslofjord. The ice maps are created manually [116].

7 Conclusion and recommendations

It is beneficial to get a good overview of the sea ice volume, the sea ice export out of the Arctic through the Fram Strait and to see how the sea ice varies inter-annually. This knowledge is of interest due to climate changes, oil and gas exploitation, ship traffic and new ship routes in the north.

This report gives a presentation of the properties of sea ice important for radar backscatter. The microwave backscatter mechanisms differ between the sea water and sea ice. Sea ice can also vary significantly in roughness, strength, salinity and thickness, imposing large variations in sea ice backscatter.

The surface's electrical characteristics, the surface's roughness, the surface's geometrical structure and the radar's incidence angle determine the radar's reflection. For sea water, the radar pulses are reflected back to the satellite from the ocean surface. The situation is different for frozen ice. The drier the ice is, the more the radar waves penetrate into the ice before being reflected back to the radar.

It has been shown that it is difficult to estimate sea ice thickness using only SAR. Some other background information is needed. SAR together with other sources is very useful.

Satellite altimetry and SAR are now being used to estimate the sea ice volume and sea ice extent in the Arctic. The estimates are validated using in situ data from ships, ice stations, upward looking sonars moored to the ocean floor and helicopters.

It is possible to measure the sea ice freeboard using a satellite altimeter, for example on ICESat and CryoSat-2. These results can be converted into sea ice thickness, and they show good agreement with in situ measurements. The data shows a decline in the sea ice volume in the Arctic over many years.

References

[1] Hendricks, S., Ricker, R., Helm, V., Haas, C., Skourup, H., Herber, A, Schwegmann, S., Gerdes, R., Davidson, M. CryoSat-2 Sea-Ice Freeboard and Thickness. ESA Living Planet Symposium, Edinburgh, 9 Sept. 2013 – 13 Sept. 2013.

[2] Ricker, R., Hendricks, S., Helm, V., Skourup, H., Davidson, M. Sensitivity of CryoSat-2 Arctic sea-ice freeboard and thickness on radar-waveform interpretation. The Cryosphere, 8, 1607-1622, 2014.

[3] Price, D., Beckers, J., Ricker, R., Kurtz, N., Rack, W., Haas, C., Helm, V., Hendricks, S., Leonard, G., Langhorne, P.J. Evaluation of CryoSat-2 derived sea-ice freeboard over fast ice in McMurdo Sound, Antarctica. Journal of Glaciology, Vol. 61, No. 226, 2015.

[4] Armitage, W.K., Ridout, A.L. Arctic sea ice freeboard from AltiKa and comparison with CryoSat-2 and Operation Ice Bridge. Geophysical Research Letters, Vol. 42, Issue 16, pp. 6724-6731, 2015.

[5] Giles, K.A., Laxon, S.W., Wingham, D.J., Wallis, D.W., Krabill, W.B., Leuschen, C.J., McAdoo, D., Manizade, S.S., Raney, R.K. Combined airborne laser and radar altimeter measurements over the Fram Strait in May 2002. Remote Sensing of Environment, Vol. 111, Issues 2-3, pp. 182-194, 2007.

[6] Laxon, S.W. et al. CryoSat-2 estimates of Arctic sea ice thickness and volume. Geophysical Research Letters 40, 732-737, 2013.

[7] Ricker, R., Hendricks, S., Beckers, J.F. The Impact of Geophysical Corrections on Sea-Ice Freeboard Retreived from Satellite Altimetry. Remote Sensing, Vol. 8, Issue 4, p. 317, 2016.

[8] Kurtz, N.T., Galin, N., Studinger, M. An improved CryoSat-2 sea ice freeboard retrieval algorithm through the use of waveform fitting. Cryosphere, Vol. 8, pp. 1217–1237, 2014.

[9] Kwok, R., Cunningham, G. Variability of Arctic sea ice thickness and volume from CryoSat-2. Philosophical Trans. Royal Society A. Mathematical, Physical and Engineering Sciences. Vol. 373, Issue 2045, 2015.

[10] Tilling, R.L., Ridout, A., Shepherd, A., Wingham, D.J. Increased Arctic sea ice volume after anomalously low melting in 2013. National Geoscience, Vol. 8, pp. 643–646, 2015.

[11] Zwally, H.J., Y. Donghui, R. Kwok, Y. Zhao. ICESat measurements of sea ice freeboard and estimates of sea ice thickness in the Weddell Sea. Journal of Geophysical Research, Vol. 113, C02S15, 2008.

[12] Assessment of research areas with great EO support potential. SIOS Deliverable D7.1. WP7: SIOS Remote sensing strategy. NERSC Technical Report no. 326. 2011.

[13] Laxon, S., et al. 2003. High interannual variability of sea ice thickness in the Arctic region. Nature, 425(6961), 947-950.

[14] Giles, K. A., S. W. Laxon, and A. L. Ridaut 2008a. Circumpolar thinning of Arctic sea ice following the 2007 record ice extent minimum. Geophys. Res. Lett., 35, L22502, doi:10.1029/2008GL035710.

[15] Kwok, R., G. F. Cunningham, M. Wensnahan, I. Rigor, H. J. Zwally, and D. Yi (2009), Thinning and volume loss of the Arctic Ocean sea ice cover: 2003-2008, J. Geophys. Res., 114, C07005, doi:10.1029/2009JC005312

[16] Richardson, C., E. Aarholt, S.-E. Hamran, P. Holmlund, and E. Isaksson (1997). Spatial Distribution of snow in western Dronning Maud Land, East Antarctica, mapped by a ground-based snow radar, J. Geophys. Res., 102, 20, 343 – 20,353.

[17] Peacock, N., and S.W. Laxon (2004). Sea surface height determination in the Arctic Ocean from ERS altimetry. J. Geophys. Res., 109, C07001, doi:10.1029/2001JC001026.

[18] Wadhams, P., W. B. Tucker III, W. B. Krabill, R. N. Swift, J. C. Comiso, and N. R. Davis (1992), Relationship between sea ice freeboard and draft in the arctic basin, and implications for ice thickness monitoring, J. Geophys. Res., 97, 20,325– 20,334.

[19] Warren, S. G., I. G. Rigor, and N. Untersteiner (1999), Snow depth on Arctic sea ice, J. Clim., 12, 1814– 1829.

[20] Renganathan, V. Arctic Sea Ice Freeboard Heights from Satellite Altimetry. Department of Geomatics Engineering, University of Calcary. January 2010.

[21] Web page accessed Aug. 30th, 2016. NOAA/NESDIS/STAR Laboratory for Satellite Altimetry. http://www.star.nesdis.noaa.gov/sod/lsa/SeaIce/background.php

[22] Renganathan, V. Arctic sea ice freeboard from ICESat altimetry. Presentation at SNAME Luncheon, October 19th, 2011.

[23] Skourup, H.: A study of Arctic sea ice freeboard heights, gravity anomalies and dynamic topography from ICESat measurements. PhD Thesis, University of Copenhagen, 2010

[24] Farrell, S. L., S. W. Laxon, D. C. McAdoo, D. Yi, and H. J. Zwally: Five years of Arctic sea ice freeboard measurements from the Ice, Cloud and land Elevation Satellite, J. Geophys. Res., 114, C04008, doi:10.1029/2008JC005074, 2009

[25] Forsberg, R. and Skourup, H. : Arctic Ocean gravity, geoid and sea ice freeboard heights from ICESat and GRACE. Geophysical Research Letters, 32(L21502), 2005

[26] Kwok, R., Cunningham, G. F., Zwally, H. J., and Yi, D.: ICESat over Arctic sea ice: Interpretation of altimetric and reflectivity profiles. Journal of Geophysical Research, 111(C06006), 2006

[27] Kwok, R., Cunningham, G. F., Zwally, H. J., and Yi, D.: Ice, Cloud, and land Elevation Satellite (ICESat) over Arctic sea ice: Retrieval of freeboard. Journal of Geophysical Research, 112(C12013), 2007

[28] Kwok, R., Zwally, H. J., and Yi, D: ICESat observations of Arctic sea ice: A first look. Geophysical Research Letters, 31(L16401), 2004

[29] Poulsen, S. K., L. Stenseng, H. Skourup, L. T. Pedersen, R. Forsberg, and L. S. Sørensen: Initial results of CryoSat-2 data from the Arctic. In proceedings CryoSat Validation Workshop, Frascati, Italy, February 1-3, 2011

[30] Skourup, H. and R. Forsberg: Sea ice freeboards from ICESat – A comparison to airborne lidar measurements. Arctic Sea Ice Thickness: Past, present and future, edited by P. Wadhams and G. Amanaditis. Climate Change and Natural Hazards Series, Brussels, 2006

[31] www.nrgan.gc.ca

[32] Olsen, R.B. Satellitter og Maritime Anvendelser. Notes for course UNIK4510, November, 2002.

[33] Sandven, S. and O. M. Johannessen, Sea ice monitoring by Remote Sensing, chapter 8, pp 241 – 283, in Remote Sensing of the Marine Environment (ed. J. Gower), Manual of Remote Sensing, Third Edition, Volume 6, Published by American Society for Photogrammetry and Remote Sensing, 2006, Maryland, USA, 338 pp.

[34] Sandven, S. et al. Assessment of research areas with great EO support potential. NERSC Technical Report no. 326. Nov. 2011.

[35] O. P. Smith. Observers guide to sea ice. Technical report, National Oceanic and Atmospheric Administration (NOAA) Ocean Service, August 2007.

[36] Manual of Standard Procedures for Observing and Reporting Ice Conditions. Canadian Ice Service, Ottawa, Ontario, Canada, 2005. ISBN: 0-660-62858-9.

[37] Moen, M.N. Analysis and Interpretation of C-band Polarimetric SAR Signatures of Sea Ice. A dissertation for the degree of Philosophiae Doctor, Nov. 2014. University of Tromsoe.

[38] Falkingham, J.C. Global satellite observation requirements for floating ice: Focusing on synthetic aperture radar. http://nsidc.org/noaa/iicwg/docs/IICWG-2014/Global-Satellite-Observation-Requirements-for-Floating-Ice-Final.pdf. Last visited in october 2014., Contract report for Environment Canada, March 2014.

[39] Wang, X., Key, J. R., & Liu, Y. (2010). A thermodynamic model for estimating sea and lake ice thickness with optical satellite data. Journal of Geophysical Research, 115 (C1203 5). doi:10.1029/2009JC005857

[40] Nakamura, K., Wakabayashi, H., Uto, S., Ushio, S., & Nishio, F. (2009). Observation of Sea-Ice Thickness Using ENVISAT Data From Lützow-Holm Bay, East Antarctica. Geoscience and Remote Sensing Letters, 6 (2), pp. 277-281.

[41] Kim, J.-W., Kim, D.-j., & Hwang, B. J. (2012). Characterization of Arctic Sea Ice Thickness Using High-Resolution Spaceborne Polarimetric SAR Data. IEEE Transactions on Geoscience and Remote Sensing, 50 (1), 13-22.

[42] Zhang, X., Zhang, J., Meng, J., & Su, T. (2013). Analysis of multi-dimensional SAR for determining the thickness of thin sea ice in the Bohai Sea. Chinese Journal of Oceanology and Limnology, 31(3), 681-698.

[43] Kwok, R., Cunningham, G. F., & Hibler, W. D. (2003). Sub-daily sea ice motion and deformation from RADARSAT observations. Geophysical Research Letters, 30 (23).

[44] Karvonen, J., Cheng, B., Vihma, T., Arkett, M., & Carrieres, T. (2012). A method for sea ice thickness and concentration analysis based on SAR data and a thermodynamic model. The Cryosphere, 6, 1507–1526.

[45] Thomas, M., Kambhamettu, C., & Geiger, C. A. (2011). Motion Tracking of Discontinuous Sea Ice. IEEE Transactions on Geoscience and Remote Sensing, 49(12), 5064-5079.

[46] Markus, T., & Cavalieri, D. J. (1998). Snow Depth Distribution Over Sea Ice in the Southern Ocean from Satellite Passive Microwave Data. In A. R. Series, Antarctic Sea Ice: Physical Processes, Interactions and Variability (pp. 19-39). American Geophysical Union.

[47] Markus, T., Cavalieri, D. J., & Ivanoff, A. (2011). Algorithm Theoretical Basis Document: Sea Ice Products: Updated December 2011. Cryospheric Sciences Laboratory, NASA Goddard Space Flight Center. Retrieved from http://nsidc.org/data/amsre/pdfs/amsr_atbd_seaice_dec2011.pdf

[48] Brucker, L., & Markus, T. (2013). Arctic-scale assessment of satellite passive microwavederived snow depth on sea ice using Operation IceBridge airborne data. J. Geophys. Res. Oceans, 118, 2892-2905. doi:10.1002/jgrc.20228

[49] Melsheimer, C. (2013). Remote Sensing of Snow Depth on Sea Ice. 2nd International Workshop on Sea Ice Concentration. Copenhagen. Retrieved February 11, 2014, from http://www.climate-cryosphere.org/media-gallery/726-2-9-melsheimer-snow-onseaice?album_id=36

[50] Fernández-Prieto, D., Hogg, A., Bamber, J., Baeseman, J., . . . Zwally, J. (2012). Earth Observation and Cryospheric Science: The Way Forward. European Space Agency. Retrieved from http://www.climate-cryosphere.org/media-gallery/824-cryospheresummary

[51] Firoozy, N., Mojabi, P., & Barber, D. (2014). Nonlinear Inversion of Arctic Snow-Covered Sea Ice Dielectric Profiles Using Microwave Scattering Data. IEEE Transactions on Geoscience and Remote Sensing, Submitted .

[52] Leinß, S., & Hajnsek, I. (2013). Snow property extraction based on polarimetry and differential SAR interferometry. Retrieved from POLINSAR 2013: https://earth.esa.int/documents/10174/409194/3_leinss_polinSAR2013_v3.pdf/b87e64b2-6fc5-4a2e-b4fc-917950ec41bf?version=1.0

[53] Lang, O., Anderssohn, J., Lumsdon, P., & Partington, K. (2013). Single pass bistatic interferometry for sea ice build-up around offshore structures. Proceedings of TanDEM-X Science Team Meeting. DLR-Oberpfaffenhofen. Retrieved from https://tandemxscience.dlr.de/

[54] Moen, M.-A., L. Ferro-Famil, A.P. Doulgeris, S.N. Anfinsen, S. Gerland and T. Eltoft: Polarimetric decomposition analysis of sea ice data, Proc. POLinSAR 2013, Frascati, Italy, 7 pp., 28 January - 1 February, 2013.

[55] S. V. Nghiem, R. Kwok, S. H. Yueh, and M. R. Drinkwater. Polarimetric signatures of sea ice: 1. theoretical model. J. Geophys. Res., 100 (C7):13681–13698, 1995.

[56] Moen, M. -A. N., Doulgeris, A. P., Anfinsen, S. N., Renner, A. H. H., Hughes, N., Gerland, S., and Eltoft, T.: Comparison of feature based segmentation of full polarimetric SAR satellite sea ice images with manually drawn ice charts, The Cryosphere, 7, 1693-1705, doi:10.5194/tc-7-1693-2013, 2013.

[57] Zhang, X., Dierking, W., Zhang, J., Meng, J. M., and Lang, H. T.: Retrieval of the thickness of undeformed sea ice from C-band compact polarimetric SAR images, The Cryosphere Discuss., 9, 5445-5483, doi:10.5194/tcd-9-5445-2015, 2015.

[58] Wadhams, P.: A comparison of sonar and laser profiles along corresponding tracks in the Arctic Ocean, in: Sea Ice Processes and Models, edited by: Pritchard, R. S., Univ. of Washington Press, Seattle, Wash., 283–299, 1980.

[59] Goebell, S.: Comparison of coincident snow-freeboard and sea ice thickness profiles derived from helicopter-borne laser altimetry and electromagnetic induction sounding, J. Geophys.Res., 116, C08018, doi:10.1029/2009JC006055, 2011.

[60] Haas, C., Gerland, S., Eicken, H., and Miller, H.: Comparison of sea-ice thickness measurements under summer and winter conditions in the Arctic using a small electromagnetic induction device, Geophysics, 62, 749–757, 1997.

[61] Wakabayashi, H., Matsuoka, T., and Nakamura, K.: Polarimetric characteristics of sea ice in the Sea of Okhotsk observed by airborne L-band SAR, IEEE T. Geosci. Remote, 42, 2412–2425, 2004.

[62] Nakamura, K.,Wakabayashi, H., Naoki, K., Nishio, F., Moriyama, T., and Uratsuka, S.: Observation of sea-ice thickness in the sea of Okhotsk by using dual-frequency and fully polarimetric airborne SAR (Pi-SAR) data, IEEE T. Geosci. Remote, 43, 2460–2469, 2005.

[63] Toyota, T., Nakamura, K., Uto, S., Ohshima, K. I., and Ebuchi, N.: Retrieval of sea ice thickness distribution in the seasonal ice zone from airborne L-band SAR, Int. J. Remote Sens., 30, 3171–3189, 2009.

[64] Liu, M., Dai, Y., Zhang, J., Zhang, X., and Meng, J.: Characterization of level sea-ice thickness in the Labrador Sea using C-band polarimetric SAR data, in: IET International Radar Conference 2013, Xi’an, China, 296–296, 2013.

[65] Accessed Feb. 16th 2016. www.asc- csa.gc.ca/eng/satellites/radarsat/description.asp

[66] Peterson, I. K., Prinsenberg, S. J., and Holladay, J. S.: Observations of sea ice thickness, surface roughness and ice motion in Amundsen Gulf, J. Geophys. Res., 113, 1–14, 2008.

[67] Hannevik, T.N.A., K. Eldhuset, and R.B. Olsen. Improving ship detection by using polarimetric decompositions. FFI-rapport 2015/01554.

[68] P.Wadhams, N. R. Davis, J. C. Comiso, R. Kutz, J. Crawford, G. Jackson, W. Krabill, C. B. Sear, R. Swift, and W. B. Tucker, III, “Concurrent remote sensing of Arctic sea ice from submarine and aircraft,” Int. J. Remote Sens., vol. 12, no. 9, pp. 1829–1840, Sep. 1991.

[69] S. Uto, T. Toyota, H. Shimoda, K. Tateyama, and K. Shirasawa, “Shipborne electromagnetic induction sounding of sea-ice thickness in the southern Sea of Okhotsk,” Ann. Glaciol., vol. 44, no. 1, pp. 253–260, Nov. 2006.

[70] R. Kwok, H. J. Zwally, and D. Yi, “ICESat observations of Arctic sea ice: A first look,” Geophys. Res. Lett., vol. 31, no. 16, p. L16 401, Aug. 2004. DOI: 10.1029/2004GL020309.

[71] R. Kwok, S. V. Nghiem, S. H. Yueh, and D. D. Huynh, “Retrieval of thin ice thickness from multifrequency polarimetric SAR data,” Remote Sens. Environ., vol. 51, no. 3, pp. 361–374, Mar. 1995.

[72] Zabel, I.H.H., K. C. Jezek, S. P. Gogineni, and P. Kanagaratnam, “Search for proxy indicators of young sea ice thickness,” J. Geophys. Res., vol. 101, no. C3, pp. 6697–6709, 1996.

[73] T. Matsuoka, S. Uratsuka, M. Satake, T. Kobayashi, A. Nadai, T. Umehara, H. Maeno, H. Wakabayashi, F. Nishio, and Y. Fukamachi, “Deriving sea-ice thickness and ice types in the Sea of Okhotsk using dual-frequency airborne SAR (Pi-SAR) data,” Ann. Glaciol., vol. 34, no. 1, pp. 429–434, Jan. 2002.

[74] F. D. Carsey, Microwave Remote Sensing of Sea Ice, vol. 68. Washington, DC: Amer. Geophys. Union, 1992.

[75] A. K. Fung and H. J. Eom, “Application of a combined rough surface and volume scattering theory to sea ice and snow backscatter,” *IEEE Trans. Geosci. Remote Sens.*, vol. GE-20, no. 4, pp. 528–536, Oct. 1982.

[76] K. Nakamura, H. Wakabayashi, S. Uto, K. Naoki, F. Nishio, and S. Uratsuka, “Sea-ice thickness retrieval in the Sea of Okhotsk using dual-polarization SAR data,” *Ann. Glaciol.*, vol. 44, no. 1, pp. 261–268, Nov. 2006.

[77] Kwok, R., Glenn F. Cunningham, Nettie LaBelle-Hamer, Benjamin Holt, Drew Rothrock. Ice Thickness derived from high-resolution radar imagery. EOS, Trans. American Geophysical Union. Vol. 80, issue 42, pp. 495-497, Oct. 19 1999.

[78] Wadhams, P., F. Parmiggiani, G. de Carolis, D. Desiderio and M.J. Doble (2004), SAR imaging of wave dispersion in Antarctic pancake ice and its use in measuring ice thickness. Geophys. Res. Lett. 31, doi:10.1029/2004GL020340

[79] Wadhams, P. and Comiso, J. C. (1992) The Ice Thickness Distribution Inferred Using Remote Sensing Techniques, in Microwave Remote Sensing of Sea Ice (ed F. D. Carsey), American Geophysical Union, Washington, D. C.. doi: 10.1029/GM068p0375

[80] Leigh, S., Z. Wang and D. Clausi. Automated ice-water classification using dual polarization SAR satellite imagery. IEEE Trans. Geosci. Remote Sens., 52(9): 5529–5539, Sept 2014.

[81] Fors, A.S., C. Brekke, S. Gerland, A.P. Doulgeris, and T. Eltoft. Extraction of Late Summer Sea Ice Properties from Polarimetric SAR Features in C- and X-band. Proceedings of PolInSAR 2015, 26-30 January 2015, Frascati, Italy.

[82] Karvonen, J.: Baltic Sea Ice Concentration Estimation Based on C-Band HH-Polarized SAR Data, IEEE Journal of Selected Topics in Applied Earth Observations and Remote Sensing, doi:10.1109/JSTARS.2012.2209199, in press, 2012c.

[83] Liu, C., J. Chao, W. Gu, Y. Xu, and F. Xie. Estimation of Sea Ice Thickness in the Bohai Sea using a Combination of VIS/NIR and SAR images. Vol. 52, No. 2, pp. 115-130. GIScience & Remote Sensing, 2015.

[84] Geldsetzer, T., and J.J. Yackel, 2009. Sea ice type and open water discrimination using dual co-polarized C-band SAR, Canadian Journal of Remote Sensing, 35(1): 73-84.

[85] Dierking, W. Sea Ice Monitoring by Synthetic Aperture Radar. Oceanography, Vol. 26, No. 2, pp. 100-111.

[86] M. Simila, J. Karvonen, C. Haas and M. Hallikainen, "C-Band SAR Based Estimation of Baltic Sea Ice Thickness Distributions," Geoscience and Remote Sensing Symposium, 2006. IGARSS 2006. IEEE International Conference on, Denver, CO, 2006, pp. 710-713.

[87] M. Mäkynen & M. Hallikainena. Investigation of C- and X-band backscattering signatures of Baltic Sea ice. Int. Journal of Remote Sensing, Vol. 25, Issue 11, pp. 2061-2086, 2004.

[88] Prinsenberg, S and I. Peterson. Identifying ice properties and ice-ocean processing with ENVISAT SAR imagery. Proc. Of Seasar 2006 Symposium, Frascati, 2006.

[89] J. Karvonen, M. Simila and I. Heiler, "Ice thickness estimation using SAR data and ice thickness history," Geoscience and Remote Sensing Symposium, 2003. IGARSS '03. Proceedings. 2003 IEEE International, 2003, pp. 74-76 vol.1.

[90] D. Haverkamp, Leen Kiat Soh and C. Tsatsoulis, "A comprehensive, automated approach to determining sea ice thickness from SAR data," in IEEE Transactions on Geoscience and Remote Sensing, vol. 33, no. 1, pp. 46-57, Jan 1995.

[91] J. A. Nystuen and F. W. Garcia, "Sea ice classification using SAR backscatter statistics," in IEEE Transactions on Geoscience and Remote Sensing, vol. 30, no. 3, pp. 502-509, May 1992.

[92] Kwok, R., E. Rignot & B. Holt. Identification of Sea Ice Types in Spaceborne Synthetic Aperture Radar Data. Journal of Geophysical Research, Vol. 97, No. C2, pp. 2391-2402, 1992.

[93] Isleifson, D., B. Hwang, D.G. Barber, R.K. Scharien, and L. Shafai. C-Band Polarimetric Backscattering Signatures of Newly Formed Sea Ice During Fall Freeze-Up. IEEE Transactions on Geoscience and Remote Sensing, Vol. 48, No. 8, Aug. 2010

[94] Yu, Y. and Rothrock, D. A.: Thin ice thickness from satellite thermal imagery, J. Geophys. Res., 101, 25753–25766, 1996.

[95] Mäkynen, M., Similä, M., and Cheng, B.: On level ice thickness retrieval in the Kara Sea using MODIS and ENVISAT ASAR data, in: Proc. of ESA Living Planet Symposium 2010, Bergen, Norway, 28 June–2 July 2010, CD ESA SP-686, 2010.

[96] Kaleschke, L., Maaß, N., Haas, C., Hendricks, S., Heygster, G., and Tonboe, R. T.: A sea-ice thickness retrieval model for 1.4 GHz radiometry and application to airborne measurements over low salinity sea-ice, The Cryosphere, 4, 583–592, doi:10.5194/tc-4-583-2010, 2010.

[97] Hallikainen, M. and D. P. Winebrenner. 1992. The physical basis for sea ice remote sensing. Chapter 3, pages 29–46 in Microwave Remote Sensing of Sea Ice, edited by F. Carsey. AGU Geophysical Monograph 68. Washington, D.C.: American Geophysical Union

[98] D. P.Winebrenner, L. D. Farmer, and I. R. Joughin, “On the response of polarimetric synthetic aperture radar signatures at 24-cm wavelength to sea ice thickness in Arctic leads,” Radio Sci., vol. 30, no. 2, pp. 373–402, 1995.

[99] Liu, M., Dai, Y., Zhang, J., Zhang, X., and Meng, J.: Characterization of level sea-ice thickness 5 in the Labrador Sea using C-band polarimetric SAR data, in: IET International Radar Conference 2013, Xi’an, China, 296–296, 2013.

[100] Makynen, M., Simila, M., Cheng, B., Laine, V., Karvonen, J. Sea Ice Thickness Retrieval in the Baltic Sea using MODIS and SAR Data. SeaSAR 2010, Proceedings of the third International Workshop held 25-29 January, 2010 at ESRIN, Frascati, Italy.

[101] Carlström, A and L.M.H. Ulander. “Validation of backscatter models for level and deformed sea ice in ERS-1 SAR images,” Int. Journal of Remote Sensing,v ol. 16,no. 7,pp. 3245-3266,1995.

[102] Makynen, M.,T . Manninen,M. Simila,J. Karvonen,M. Hallikainen. “Incidence Angle Dependence of the Statistical Properties of C-Band HH-Polarization Backscattering Signatures of the Baltic Sea Ice”,IEEE Transactions on Geoscience and Remote Sensing,v 40,n 12,pp 2593-2605,2002.

[103] Ball, G. H., D. J. Hall. “ISOD ATA,an Iterative Method of Multivariate Analysis and Pattern Recognition”, Proc. IEEE Int. Commnunications Conference,1966.

[104] Linde, Y ., Buzo,A.,and Gray,R. M. (1980). An algorithm for vector quantizer design. IEEE Transactions on Communication,v 28,n 1,pp 84-95,1980.

[105] Drinkwater, M.., Kwok, R., Winebrenner, D.P. and Rignot, E. Multifrequency polarimetric synthetic aperture radar observations of sea ice. Journal of Geophysical Research, Vol. 96, No. C11, pp. 20 679 – 20 698, 1991.

[106] Shokr, M. and Sinha, N.K.Arctic sea ice microstructure observations relevant to microwave scattering. Arctic, Vol. 47, No. 3, pp. 265-279, 1994.

[107] Drinkwater, M.R. and Crocker, G.B. Modeling changes in the dielectric and scattering properties of young snow-covered sea ice at GHz frequencies. Journal of Glaciology, Vol. 34, No. 118, pp. 274-282, 1988.

[108] Barber, D.G., Fung, A.K., Grenfell, T.C., Nghiem, S.V., Onstott, R.G., Lytle, V.I. et al. The role of snow on microwave emission and scattering over first-year sea ice. IEEE Transactions on Geoscience and Remote Sensning, Vol. 36, No. 5, pp. 1750-1763, 1998.

[109] https://www.ec.gc.ca/glaces-ice/default.asp?lang=En&n=D5F7EA14-1&offset=1&toc=hide. Canadian Ice Service. Accessed September 2016.

[110] Shuchman, R.A., Onstott, R.G., Johannessen, O.M., Sandven, S. and Johannessen, J.A. Chapter 18. Processes at the Ice Edge – The Arctic. Part of Synthetic Aperture Radar Marine User’s Manual.C.R Jackson and J.R. Apel. US Department of Commerce, NOAA, 2004.

[111] Kwok, R. PhD, Senior research Scientist, Jet Propulsion Laboratory. Communication via e-mail May 2016.

[112] Karvonen, J. Finnish Meteorological Institute. Communication via e-mail May 2016.

[113] Moen, M.-A. Communication via e-mail February 2016.

[114] Langlois, D. Communication via e-mail May 2016. .

[115] Holden, T. Communication via e-mail May 2016.

[116] kystverket.no. Accessed May 2015.

[117] www.nersc.no/project/coresat. Nansen Environmental and Remote Sensing Center. Accessed September 2016.

About FFI

The Norwegian Defence Research Establishment (FFI) was founded 11th of April 1946. It is organised as an administrative agency subordinate to the Ministry of Defence.

FFI's MISSION

FFI is the prime institution responsible for defence related research in Norway. Its principal mission is to carry out research and development to meet the requirements of the Armed Forces. FFI has the role of chief adviser to the political and military leadership. In particular, the institute shall focus on aspects of the development in science and technology that can influence our security policy or defence planning.

FFI's VISION

FFI turns knowledge and ideas into an efficient defence.

FFI's CHARACTERISTICS

Creative, daring, broad-minded and responsible.

Om FFI

Forsvarets forskningsinstitutt ble etablert 11. april 1946. Instituttet er organisert som et forvaltningsorgan med særskilte fullmakter underlagt Forsvarsdepartementet.

FFIs FORMÅL

Forsvarets forskningsinstitutt er Forsvarets sentrale forskningsinstitusjon og har som formål å drive forskning og utvikling for Forsvarets behov. Videre er FFI rådgiver overfor Forsvarets strategiske ledelse. Spesielt skal instituttet følge opp trekk ved vitenskapelig og militærteknisk utvikling som kan påvirke forutsetningene for sikkerhetspolitikken eller forsvarsplanleggingen.

FFIs VISJON

FFI gjør kunnskap og ideer til et effektivt forsvar.

FFIs VERDIER

Skapende, drivende, vidsynt og ansvarlig.

FFI's organisation

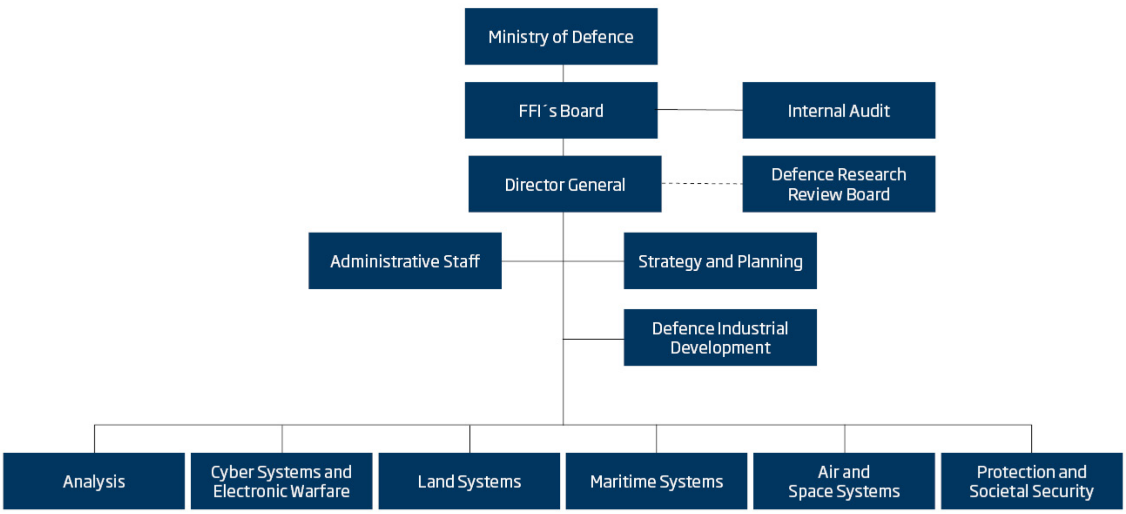

Forsvarets forskningsinstitutt
Postboks 25
2027 Kjeller

Besøksadresse:
Instituttveien 20
2007 Kjeller

Telefon: 63 80 70 00
Telefaks: 63 80 71 15
Epost: ffi@ffi.no

Norwegian Defence Research Establishment (FFI)
P.O. Box 25
NO-2027 Kjeller

Office address:
Instituttveien 20
N-2007 Kjeller

Telephone: +47 63 80 70 00
Telefax: +47 63 80 71 15
Email: ffi@ffi.no

FFI Forsvarets forskningsinstitutt
Norwegian Defence Research Establishment